Engineering with Computers (2022) 38:2361–2384
https://doi.org/10.1007/s00366-020-01206-5

ORIGINAL ARTICLE

On the vibration of nanobeams with consistent two-phase nonlocal strain gradient theory: exact solution and integral nonlocal finite-element model

Mahmood Fakher[1] · **Shahrokh Hosseini-Hashemi**[1,2]

Received: 6 August 2020 / Accepted: 23 October 2020 / Published online: 15 November 2020
© Springer-Verlag London Ltd., part of Springer Nature 2020

Abstract

Recently, it has been proved that the common nonlocal strain gradient theory has inconsistence behaviors. The order of the differential nonlocal strain gradient governing equations is less than the number of all mandatory boundary conditions, and therefore, there is no solution for these differential equations. Given these, for the first time, transverse vibrations of nanobeams are analyzed within the framework of the two-phase local/nonlocal strain gradient (LNSG) theory, and to this aim, the exact solution as well as finite-element model are presented. To achieve the exact solution, the governing differential equations of LNSG nanobeams are derived by transformation of the basic integral form of the LNSG to its equal differential form. Furthermore, on the basis of the integral LNSG, a shear-locking-free finite-element (FE) model of the LNSG Timoshenko beams is constructed by introducing a new efficient higher order beam element with simple shape functions which can consider the influence of strains gradient as well as maintain the shear-locking-free property. Agreement between the exact results obtained from the differential LNSG and those of the FE model, integral LNSG, reveals that the LNSG is consistent and can be utilized instead of the common nonlocal strain gradient elasticity theory.

Keywords Two-phase local/nonlocal strain gradient · Exact solution · Finite-element method · Euler–Bernoulli · Timoshenko · Shear-locking · Vibration

1 Introduction

Due to paradoxical behaviors [1–4] of the common differential nonlocal elasticity [5–8] which has been widely utilized by researchers to consider the size effects for studying the mechanics of nano structures [9–15], other size-dependent elasticity theories such as stress-driven integral nonlocal [16, 17] and two-phase local/nonlocal have been recently attracted the attentions of the nano-mechanic researchers.

Although, some valuable efforts [18, 19] have been made to resolve the weakness of the differential nonlocal, it has been indicated [20, 21] that using the differential form of nonlocal elasticity instead of its integral form is allowable only in a few certain cases in which satisfying additional constitutive boundary conditions (CBCs), resulted from this transformation, is possible.

It should be noted that the integral form of nonlocal elasticity has been seldom used in the past years [22–24], while after presentation of Ref.[20], a significant growth occurs in applying the integral form of nonlocal theory. Due to this fact, the basic integral form of pure nonlocal elasticity has been directly employed to probe into the static bending [25], vibration characteristics, and buckling [26] of Euler–Bernoulli nanobeams without any paradoxes. In these two works, the Laplace transform method has been applied to present an analytical solution which has led to some comments [27] and replies [28] about the correctness of the proposed exact solution. In addition, the integral nonlocal finite-element method (FEM) has been employed to examine the nonlocal characteristics of Euler–Bernoulli nanobeams [29–31]. Also, the vibration frequency shifts resulted from the attached mass on a cantilever carbon-nanotube sensor [32] have been predicted by the integral nonlocal FEM. To

✉ Mahmood Fakher
fakher@mecheng.iust.ac.ir

1 School of Mechanical Engineering, Iran University of Science and Technology, Narmak, 16846-13114 Tehran, Iran

2 Center of Excellence in Railway Transportation, Iran University of Science and Technology, Narmak, 16842-13114 Tehran, Iran

analyze the nonlocal static bending of Timoshenko nanobeams [33], an integral nonlocal FEM model has been constructed using a higher order beam element with eight nodes to avoid the shear-locking effect. Along these works, it can be pointed to the papers in which the isogeometric analysis [34–36] as well as FEM [37, 38] have been developed within the framework of the integral nonlocal and strain gradient elasticity theories.

Applying two-phase local/nonlocal elasticity, for considering the nonlocal effects in nanostructures, has been recently proposed by researchers due to its advantages over the common differential nonlocal. Being paradox free, compatibility between the results extracted from the differential form with those obtained by the integral form, and compatibility between the order of the differential governing equations and the number of boundary conditions are some of these advantages. However, it is noted that employing two-phase elasticity instead of the differential nonlocal increases the complexity of the problems, so that finding efficient solutions is now an important challenge.

On the basis of the two-phase elasticity, nonlocal bending analysis of nanobeams has been performed and associated exact solutions have been presented for the Euler–Bernoulli [39] and Timoshenko nanobeams [40]. Also, different mechanical characteristics of nanostructures such as axial, torsional, and transverse vibrations of nanorods [41], nanobeams [42, 43], and double nanobeams system [44] have been evaluated by developing the exact solutions [41–43] as well as numerical methods such as FEM [43] and generalize differential quadrature method (GDQM) [44]. To utilize the advantages of two-phase elasticity, size dependence of elastic medium and axial loads, resulted from the thermal expansion and nonlinear van-Karman strain, has been considered by two-phase elasticity and their influences on the linear [45] and nonlinear [46] vibrations of nanobeams have been investigated. In addition, by combination of surface and two-phase elasticity theories, the damping vibrations of local/nonlocal nanobeams [47] have been studied. Assessment of the complex natural frequencies obtained by exact solution indicated that using the local/nonlocal theory eliminates the paradoxes in both of the real and imaginary parts of vibration frequencies. Also, size-dependent coupled flexural–axial vibrations of cantilevered mass nanosensors [48] have been investigated by two-phase elasticity to prevent the paradoxical behavior due to applying differential nonlocal on clamped-free beams.

In addition to the common differential nonlocal, the nonlocal strain gradient elasticity, introduced by Lim et al. [49], has been widely utilized [50–52] by researchers to explore on the size-dependent mechanics of various nanostructures. For instance, wave propagation [49, 53–55], longitudinal vibration [56], bending, buckling, and transverse vibrations [57, 58] of nanobeams and nanoplates have been comprehensively studied in the recent years by using this theory.

Here, it is essential to express that the nonlocal strain gradient is resulted from the combination of integral nonlocal theory with the strain gradient one and its differential form has been considered in most works without paying attention to this fact that the transformation of integral nonlocal strain gradient to a differential form is allowable if the CBCs related to this conversion can be satisfied. This common negligence leads to significant differences [59] between the results of the differential nonlocal strain gradient and those that have been extracted by the integral nonlocal strain gradient. Despite the suggestion [60] of satisfying the CBCs, resulted from conversion of the integral nonlocal strain gradient to the differential form, instead of the higher order boundary conditions related to the strain gradient theory, inconsistency of this theory has been proved [61, 62] and it has been shown that achieving to correct results from the differential nonlocal strain gradient is impossible, and therefore, using the common differential form of nonlocal strain gradient theory is not correct. To present more explanations about this issue, it should be said that the order of the differential governing equations derived by the nonlocal strain gradient is less than the number of all boundary conditions and these differential equations have no solution at all. To resolve these issues, the two-phase local/nonlocal strain gradient (LNSG) theory has been utilized to extract the closed-form solutions for the static deflections of nanorods subjected to a tensional force [63] and, for studying the size-dependent longitudinal vibrations of nano-scaled rods [64].

According to these facts, in this work, free transverse vibrations of nanobeams are analyzed on the basis of the LNSG, for the first time. By transformation of the integral form of LNSG to the equal differential form, the differential equations associated with the LNSG Euler–Bernoulli and Timoshenko nanobeams as well as all mandatory CBCs are derived, and then, the exact solutions are presented by satisfying all BCs. In addition, by introducing a new higher order shear-locking-free beam element and using the basic integral form of LNSG, the FE model of LNSG Timoshenko nanobeams is constructed with the aim of preventing shear-locking effect without increasing the complexity of the integral nonlocal strain gradient FE model. It is shown that employing the LNSG makes it possible to obtain solvable differential equations with the order equal to the number of all mandatory BCs. Also, compatibly between the exact results obtained by solving the differential LNSG with those of the integral LNSG FE model reconfirms the consistency of the LNSG theory.

2 Problem formulation

To apply the LNSG elasticity for recognizing the size-dependent vibration characteristics of nanobeams, the differential governing equations, all constitutive boundary conditions, and exact solutions will be derived using the equal differential form of LNSG. To provide a comprehensive study, the formulations associated with the Euler–Bernoulli beam theory (EBT) as well as Timoshenko beam theory (TBT) are presented in the following.

Furthermore, the finite-element model of LNSG Timoshenko beam is constructed using a new efficient higher order locking-free beam element and direct use of the integral form of LNSG. To this aim, a beam is assumed with the length of L and cross section with the height of h and width of b which they are respectively located along the x-, z-, and y-directions of the Cartesian coordinates, see Fig. 1.

2.1 Two-phase local/nonlocal strain gradient

First, the corresponding local/nonlocal stress relations of LNSG nanobeams are presented as follow using the local stresses, $\sigma_{\mathrm{kl}}^{\mathrm{local}}$, due to local strains, and the higher order ones, $\sigma_{\mathrm{kl}}^{1\ \mathrm{local}}$, resulted from the strain gradient [63, 64]:

$$\sigma_{\mathrm{kl}}(x) = \zeta_1 \sigma_{\mathrm{kl}}^{\mathrm{local}}(x) + \zeta_2 \int_L \alpha\left(\left|x - x'\right|, k\right)\sigma_{\mathrm{kl}}^{\mathrm{local}}\left(x'\right)dx'$$
$$\sigma_{\mathrm{kl}}^{1}(x) = \zeta_1 \sigma_{\mathrm{kl}}^{1\ \mathrm{local}}(x) + \zeta_2 \int_L \alpha\left(\left|x - x'\right|, k\right)\sigma_{\mathrm{kl}}^{1\ \mathrm{local}}\left(x'\right)dx'$$
$$\zeta_1 > 0,\ \zeta_2 > 0,\ \zeta_1 + \zeta_2 = 1 \text{ and } \alpha\left(\left|x - x'\right|, k\right) = \frac{1}{2k}e^{-\frac{|x-\bar{x}|}{k}}, \tag{1}$$

where ζ_1, ζ_2, and k, indicate the local phase fraction factor, nonlocal phase fraction factor, and nonlocal parameter, respectively. In addition, $\alpha\left(|x - x'|, k\right)$ is nonlocal kernel function. Also, it has been shown [42, 65] that the following integral equation, i.e., Eq. (2), can be replaced with an equal differential equation, i.e., Eq. (3), by satisfying essential CBCs, i.e., Eq. (4):

$$\mathfrak{R}(x) = \mathfrak{J}(x) + C\int_0^L e^{\vartheta|x-\bar{x}|}\mathfrak{J}\left(\bar{x}\right)d\bar{x}. \tag{2}$$

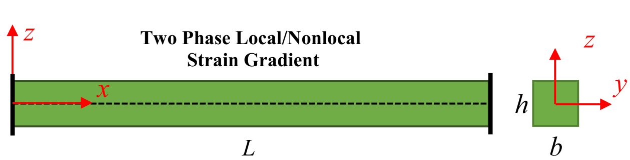

Fig. 1 Schematic of problem

$$\mathfrak{R}''(x) - \vartheta^2\mathfrak{R}(x) = \mathfrak{J}''(x) + \vartheta(2C - \vartheta)\mathfrak{J}(x). \tag{3}$$

$$\begin{aligned}\mathfrak{R}'(x) + \vartheta\,\mathfrak{R}(x) &= \mathfrak{J}'(x) + \vartheta\mathfrak{J}(x) \quad \text{at } x = 0\\ \mathfrak{R}'(x) - \vartheta\,\mathfrak{R}(x) &= \mathfrak{J}'(x) - \vartheta\mathfrak{J}(x) \quad \text{at } x = L.\end{aligned} \tag{4}$$

2.2 Governing equations of EBT

To extract the equations governed on the EBT within the framework of the LNSG, the displacement field is considered as follows:

$$u_1^E = -z\frac{\partial w^E(x,t)}{\partial x},\ u_2^E = w^E(x,t),\ u_3^E = 0, \tag{5}$$

where u_1^E, u_2^E, and u_3^E are the deflections in the x-, y-, and z-directions, respectively. Also, the superscript "E" refers to the EBT and $w^E(x,t)$ is the transverse displacement of the neutral axis. Next, the axial strain related to the EBT is presented:

$$\varepsilon_{xx}^E = -z\frac{\partial^2 w^E}{\partial x^2}. \tag{6}$$

According to Eq. (1), the LNSG stress–strain relations can be obtained for EBT:

$$\begin{aligned}\sigma_{xx}^E &= \zeta_1 E\varepsilon_{xx}^E + \frac{\left(1-\zeta_1\right)}{2k}E\int_0^L e^{-\frac{|x-\bar{x}|}{k}}\varepsilon_{xx}^E(\bar{x})d\bar{x}\\ \sigma_{xx}^{E1} &= l_m^2\zeta_1 E\varepsilon_{xx,x}^E + \frac{l_m^2\left(1-\zeta_1\right)}{2k}E\int_0^L e^{-\frac{|x-\bar{x}|}{k}}\varepsilon_{xx,x}^E(\bar{x})d\bar{x},\end{aligned} \tag{7}$$

where l_m and E indicate the length scale of the strain gradient and Young modulus, respectively. By employing the integration by parts method, the variation of the strain potential is written as:

$$\begin{aligned}\delta U^E &= \int_V \left[\sigma_{xx}^E\delta\varepsilon_{xx}^E + \sigma_{xx}^{E1}\delta\varepsilon_{xx,x}^E\right]dAdx\\ \delta U^E &= \int_V \left(\sigma_{xx}^E - \frac{d}{dx}\sigma_{xx}^{E1}\right)\delta\varepsilon_{xx}^E dAdx + \left[\int_A \sigma_{xx}^{E1}\delta\varepsilon_{xx}^E dA\right]_0^L\\ t_{xx}^E &= \sigma_{xx}^E - \frac{d}{dx}\sigma_{xx}^{E1};\quad \sigma_{xx}^{E1}\delta\varepsilon_{xx}^E\Big|_0^L = 0.\end{aligned} \tag{8}$$

According to Eq. (8), it can be expressed that the stress of LNSG is resulted from the σ_{xx}^E and the first derivative of the σ_{xx}^{E1} by satisfying the strain gradient boundary conditions, i.e., $\sigma_{xx}^{E1}\delta\varepsilon_{xx}^E\big|_0^L = 0$. Given this, the LNSG bending moment of EBT is obtained as Eq. (9) in which A and I stand for the area and the moment of inertia of cross section, respectively:

$$M^E = -\zeta_1 EI \frac{\partial^2 w^E}{\partial x^2} - \frac{\zeta_2}{2k} EI \int_0^L e^{-\frac{|x-\bar{x}|}{k}} \frac{\partial^2 w^E}{\partial \bar{x}^2} d\bar{x} + \zeta_1 EI l_m^2 \frac{\partial^4 w^E}{\partial x^4} + \frac{\zeta_2}{2k} EI l_m^2 \frac{d}{dx} \left[\int_0^L e^{-\frac{|x-\bar{x}|}{k}} \frac{\partial^3 w^E}{\partial \bar{x}^3} d\bar{x} \right]. \tag{9}$$

To transform this complex differential-integral equation, i.e., Eq. (9), into an equal differential form, it is essential to rewrite this equation with the help of the procedure presented in [63]. Therefore, the following relation is considered:

$$\frac{d}{dx} \left[\int_0^L e^{-\frac{|x-\bar{x}|}{k}} \frac{\partial^3 w^E}{\partial \bar{x}^3} d\bar{x} \right] = -\frac{2}{k} \frac{\partial^2 w^E}{\partial x^2} + \frac{1}{k^2} \left[\int_0^L e^{-\frac{|x-\bar{x}|}{k}} \frac{\partial^2 w^E}{\partial \bar{x}^2} d\bar{x} \right] + \frac{1}{k} \left(\frac{\partial^2 w^E}{\partial x^2}(0) e^{-\frac{x}{k}} + \frac{\partial^2 w^E}{\partial x^2}(L) e^{\frac{x-L}{k}} \right). \tag{10}$$

And, to summarize the following equations, Eq. (11) is presented:

$$\frac{\partial^2 w^E}{\partial x^2}(0) = St_1^E, \quad \frac{\partial^2 w^E}{\partial x^2}(L) = St_2^E. \tag{11}$$

Now, by applying Eqs (10) and (11), Eq. (9) can be rewritten as Eq. (12):

$$M^E = -EI \left(\zeta_1 + \frac{(1-\zeta_1) l_m^2}{k^2} \right) \frac{\partial^2 w^E}{\partial x^2} - \frac{EI}{2k} \left(1 - \frac{l_m^2}{k^2} \right) (1-\zeta_1) \int_0^L e^{-\frac{|x-\bar{x}|}{k}} \frac{\partial^2 w^E}{\partial \bar{x}^2} d\bar{x} + \zeta_1 EI l_m^2 \frac{\partial^4 w^E}{\partial x^4} + \frac{(1-\zeta_1)}{2k^2} EI\, l_m^2 \left(St_1^E e^{-\frac{x}{k}} + St_2^E e^{\frac{x-L}{k}} \right). \tag{12}$$

Here, the following relations are represented:

$$\mu_1^E = EI \left(\zeta_1 + \frac{(1-\zeta_1) l_m^2}{k^2} \right), \quad \mu_2^E = \frac{EI}{2k} \left(1 - \frac{l_m^2}{k^2} \right) (1-\zeta_1)$$
$$\mu_3^E = -\zeta_1 EI l_m^2, \quad \mu_4^E = -\frac{EI}{2} \frac{l_m^2}{k^2} (1-\zeta_1), \quad \mu_5^E = St_1^E e^{-\frac{x}{k}} + St_2^E e^{\frac{x-L}{k}}. \tag{13}$$

Now, Eq. (12) can be rewritten by utilizing Eq. (13):

$$\frac{M^E}{\mu_1^E} + \frac{\mu_3^E}{\mu_1^E} \frac{\partial^4 w^E}{\partial x^4} - \frac{\mu_4^E}{\mu_1^E} \mu_5^E = -\frac{\partial^2 w^E}{\partial x^2} - \frac{\mu_2^E}{\mu_1^E} \int_0^L e^{-\frac{|x-\bar{x}|}{k}} \frac{\partial^2 w^E}{\partial \bar{x}^2} d\bar{x}. \tag{14}$$

It can be seen that Eq. (14) is obtained in the form of Eq. (2), and therefore, the equal differential form of this integral–differential equation can be generated using Eq. (3):

$$\frac{1}{\mu_1^E} \frac{\partial^2 M^E}{\partial x^2} + \frac{\mu_3^E}{\mu_1^E} \frac{\partial^6 w^E}{\partial x^6} - \frac{1}{k^2} \left[\frac{M^E}{\mu_1^E} + \frac{\mu_3^E}{\mu_1^E} \frac{\partial^4 w^E}{\partial x^4} \right] = -\frac{\partial^4 w^E}{\partial x^4} + \frac{1}{k} \left(\frac{2\mu_2^E}{\mu_1^E} + \frac{1}{k} \right) \frac{\partial^2 w^E}{\partial x^2}. \tag{15}$$

In addition, as previously mentioned, it is essential to satisfy the CBCs associated with the LNSG bending moment of EBT if Eq. (14) is replaced with Eq. (15). Therefore, according to the Eqs.(4) and (5), two CBCs can be extracted from Eq. (14):

$$\begin{aligned}
&\frac{1}{\mu_1^E} \frac{\partial M^E}{\partial x} + \frac{\mu_3^E}{\mu_1^E} \frac{\partial^5 w^E}{\partial x^5} - \frac{\mu_4^E}{\mu_1^E} \frac{\partial \mu_5^E}{\partial x} - \frac{1}{k} \left[\frac{M^E}{\mu_1^E} + \frac{\mu_3^E}{\mu_1^E} \frac{\partial^4 w^E}{\partial x^4} - \frac{\mu_4^E}{\mu_1^E} \mu_5^E \right] = -\frac{\partial^3 w^E}{\partial x^3} + \frac{1}{k} \frac{\partial^2 w^E}{\partial x^2} \quad at\, x = 0 \\
&\frac{1}{\mu_1^E} \frac{\partial M^E}{\partial x} + \frac{\mu_3^E}{\mu_1^E} \frac{\partial^5 w^E}{\partial x^5} - \frac{\mu_4^E}{\mu_1^E} \frac{\partial \mu_5^E}{\partial x} + \frac{1}{k} \left[\frac{M^E}{\mu_1^E} + \frac{\mu_3^E}{\mu_1^E} \frac{\partial^4 w^E}{\partial x^4} - \frac{\mu_4^E}{\mu_1^E} \mu_5^E \right] = -\frac{\partial^3 w^E}{\partial x^3} - \frac{1}{k} \frac{\partial^2 w^E}{\partial x^2} \quad at\, x = L.
\end{aligned} \tag{16}$$

In this step, the equilibrium equations of EBT are represented:

$$\begin{aligned}
&\frac{\partial^2 M^E}{\partial x^2} - m_1 \frac{\partial^2 w^E}{\partial t^2} = 0 \\
&Q^E = \frac{\partial M^E}{\partial x} \\
&m_1 = \rho A,
\end{aligned} \tag{17}$$

where ρ is the mass density. Next, the first part of Eq. (17) is substituted into Eq. (15) and the LNSG bending moment of EBT is obtained. Also, the shear force of EBT, which should be utilized for satisfying the boundary conditions related to the beams with free ends, is written using the second part of Eq. (17):

$$M^E = k^2\mu_3^E \frac{\partial^6 w^E}{\partial x^6} - \left(\mu_3^E - k^2\mu_1^E\right)\frac{\partial^4 w^E}{\partial x^4} - \left(2\mu_2^E k + \mu_1^E\right)\frac{\partial^2 w^E}{\partial x^2} + k^2 m_1 \frac{\partial^2 w^E}{\partial t^2}$$

$$Q^E = k^2\mu_3^E \frac{\partial^7 w^E}{\partial x^7} - \left(\mu_3^E - k^2\mu_1^E\right)\frac{\partial^5 w^E}{\partial x^5} - \left(2\mu_2^E k + \mu_1^E\right)\frac{\partial^3 w^E}{\partial x^3} + k^2 m_1 \frac{\partial^3 w^E}{\partial x \partial t^2}. \tag{18}$$

Now that the differential form of the LNSG bending moment is available, it is possible to obtain the differential governing equation of EBT by substituting the first part of Eq. (18) into the first part of Eq. (17):

$$k^2\mu_3^E \frac{\partial^8 w^E}{\partial x^8} - \left(\mu_3^E - k^2\mu_1^E\right)\frac{\partial^6 w^E}{\partial x^6} - \left(2\mu_2^E k + \mu_1^E\right)\frac{\partial^4 w^E}{\partial x^4} + k^2 m_1 \frac{\partial^4 w^E}{\partial x^2 \partial t^2} - m_1 \frac{\partial^2 w^E}{\partial t^2} = 0. \tag{19}$$

Also, the CBCs presented in Eq. (16) should be obtained in term of w^E by substituting the differential form of M^E, Eq. (18), into Eq. (16).

2.3 Governing equations of TBT

To derive the TBT governing equations using the LNSG elasticity theory, the displacements of Timoshenko beams are written in terms of the transverse, $w^T(x,t)$, and rotational deflections, $\phi(x,t)$, of the neutral axis:

$$u_1^T = z\phi(x,t),\ \ u_2^T = w^T(x,t),\ \ u_3^T = 0. \tag{20}$$

Also, the nonzero strains are achieved using Eq. (20):

$$\varepsilon_{xx}^T = z\frac{\partial \phi}{\partial x},\ \gamma_{xz} = \frac{\partial w^T}{\partial x} + \phi. \tag{21}$$

By utilizing Eq. (1) as well as Eq. (21), the stress–strain relations corresponding to the TBT can be obtained as follows:

$$\begin{aligned}
\sigma_{xx}^T &= \zeta_1 E\varepsilon_{xx}^T + \frac{\left(1-\zeta_1\right)}{2k}E\int_0^L e^{-\frac{|x-\bar{x}|}{k}}\varepsilon_{xx}^T(\bar{x})d\bar{x}\\
\sigma_{xx}^{T1} &= l_m^2\zeta_1 E\varepsilon_{xx,x}^T + \frac{l_m^2\left(1-\zeta_1\right)}{2k}E\int_0^L e^{-\frac{|x-\bar{x}|}{k}}\varepsilon_{xx,x}^T(\bar{x})d\bar{x}\\
\sigma_{xz} &= \zeta_1 G\gamma_{xz} + \frac{\left(1-\zeta_1\right)}{2k}G\int_0^L e^{-\frac{|x-\bar{x}|}{k}}\gamma_{xz}(\bar{x})d\bar{x}\\
\sigma_{xz}^1 &= l_m^2\zeta_1 G\gamma_{xz,x} + \frac{l_m^2\left(1-\zeta_1\right)}{2k}G\int_0^L e^{-\frac{|x-\bar{x}|}{k}}\gamma_{xz,x}(\bar{x})d\bar{x}.
\end{aligned} \tag{22}$$

Here, G shows the shear modulus. In this step, variations of the strain potential are written using the integration by parts method:

$$\delta U^T = \int_V \left[\sigma_{xx}^T\delta\varepsilon_{xx}^T + \sigma_{xx}^{T1}\delta\varepsilon_{xx,x}^T + \sigma_{xz}\delta\gamma_{xz} + \sigma_{xz}^1\delta\gamma_{xz,x}\right]dAdx$$

$$\delta U^T = \int_V \left(\sigma_{xx}^T - \frac{d}{dx}\sigma_{xx}^{T1}\right)\delta\varepsilon_{xx}^T dAdx + \int_V \left(\sigma_{xz} - \frac{d}{dx}\sigma_{xz}^1\right)\delta\gamma_{xz}dAdx + \left[\int_A \sigma_{xx}^{T1}\delta\varepsilon_{xx}^T dA\right]_0^L + \left[\int_A \sigma_{xz}^1\delta\gamma_{xz}dA\right]_0^L$$

$$\begin{aligned}
t_{xx}^T &= \sigma_{xx}^T - \frac{d}{dx}\sigma_{xx}^{T1};\ \ \sigma_{xx}^{T1}\delta\varepsilon_{xx}^T\Big|_0^L = 0\\
t_{xz} &= \sigma_{xz} - \frac{d}{dx}\sigma_{xz}^1;\ \ \sigma_{xz}^1\delta\gamma_{xz}\Big|_0^L = 0.
\end{aligned} \tag{23}$$

According to Eq. (21), Eq. (22), and Eq. (23), the LNSG bending moment and shear force of Timoshenko nanobeams are generated as Eq. (24):

$$M^T = \zeta_1 EI\frac{\partial\phi}{\partial x} + \frac{\zeta_2}{2k}EI\int_0^L e^{-\frac{|x-\bar{x}|}{k}}\frac{\partial\phi}{\partial\bar{x}}d\bar{x} - \zeta_1 EIl_m^2\frac{\partial^3\phi}{\partial x^3} - \frac{\zeta_2}{2k}EIl_m^2\frac{d}{dx}\left[\int_0^L e^{-\frac{|x-\bar{x}|}{k}}\frac{\partial^2\phi}{\partial\bar{x}^2}d\bar{x}\right]$$

$$Q^T = \zeta_1 K_s GA\left(\frac{\partial w^T}{\partial x} + \phi\right) + \frac{\zeta_2}{2k}K_s GA\int_0^L e^{-\frac{|x-\bar{x}|}{k}}\left(\frac{\partial w^T}{\partial\bar{x}} + \phi\right)d\bar{x} - \zeta_1 K_s GAl_m^2\left(\frac{\partial^3 w^T}{\partial x^3} + \frac{\partial^2\phi}{\partial x^2}\right) - \frac{\zeta_2}{2k}K_s GAl_m^2\frac{d}{dx}\left[\int_0^L e^{-\frac{|x-\bar{x}|}{k}}\left(\frac{\partial^2 w^T}{\partial\bar{x}^2} + \frac{\partial\phi}{\partial\bar{x}}\right)d\bar{x}\right]. \tag{24}$$

Here, K_s is the shear correction factor. In this step, the following relations are presented:

$$\frac{d}{dx}\left[\int_0^L e^{-\frac{|x-\bar{x}|}{k}}\frac{\partial^2\phi}{\partial\bar{x}^2}d\bar{x}\right]=-\frac{2}{k}\frac{\partial\phi}{\partial x}+\frac{1}{k^2}\left[\int_0^L e^{-\frac{|x-\bar{x}|}{k}}\frac{\partial\phi}{\partial\bar{x}}d\bar{x}\right]+ +\frac{1}{k}\left(\frac{\partial\phi}{\partial x}(0)e^{-\frac{x}{k}}+\frac{\partial\phi}{\partial x}(L)e^{\frac{x-L}{k}}\right) \tag{25}$$

$$\frac{d}{dx}\left[\int_0^L e^{-\frac{|x-\bar{x}|}{k}}\left(\frac{\partial^2 w^T}{\partial\bar{x}^2}+\frac{\partial\phi}{\partial\bar{x}}\right)d\bar{x}\right]=-\frac{2}{k}\left(\frac{\partial w^T}{\partial x}+\phi\right) +\frac{1}{k^2}\left[\int_0^L e^{-\frac{|x-\bar{x}|}{k}}\left(\frac{\partial w^T}{\partial\bar{x}}+\phi\right)d\bar{x}\right]+ +\frac{1}{k}\left(\left(\frac{\partial w^T}{\partial x}+\phi\right)(0)e^{-\frac{x}{k}}+\left(\frac{\partial w^T}{\partial x}+\phi\right)(L)e^{\frac{x-L}{k}}\right). \tag{26}$$

Next, to brevity, it is assumed that:

$$\frac{\partial\phi}{\partial x}(0)=St_1^T,\ \frac{\partial\phi}{\partial x}(L)=St_2^T \qquad \left(\frac{\partial w^T}{\partial x}+\phi\right)(0)=St_3^T,\ \left(\frac{\partial w^T}{\partial x}+\phi\right)(L)=St_4^T. \tag{27}$$

Substituting Eq. (27) into Eqs. (25), (26) and then into Eq. (24) gives:

$$\mu_1^T=EI\left(\zeta_1+\frac{(1-\zeta_1)l_m^2}{k^2}\right),\ \mu_2^T=\frac{EI}{2k}\left(1-\frac{l_m^2}{k^2}\right)(1-\zeta_1)$$
$$\mu_3^T=-\zeta_1 EIl_m^2,\ \mu_4^T=-\frac{EI}{2}\frac{l_m^2}{k^2}(1-\zeta_1),\quad \mu_5^T=St_1^Te^{-\frac{x}{k}}+St_2^Te^{\frac{x-L}{k}}$$
$$\eta_1=K_sGA\left(\zeta_1+\frac{(1-\zeta_1)l_m^2}{k^2}\right),\ \eta_2=\frac{K_sGA}{2k}\left(1-\frac{l_m^2}{k^2}\right)(1-\zeta_1)$$
$$\eta_3=-\zeta_1K_sGAl_m^2,\eta_4=-\frac{K_sGA}{2}\frac{l_m^2}{k^2}(1-\zeta_1),\quad \eta_5=St_3^Te^{-\frac{x}{k}}+St_4^Te^{\frac{x-L}{k}}. \tag{29}$$

By employing the symbols presented in Eq. (29), Eq. (28) is rewritten as follows:

$$\frac{M^T}{\mu_1^T}-\frac{\mu_3^T}{\mu_1^T}\frac{\partial^3\phi}{\partial x^3}-\frac{\mu_4^T}{\mu_1^T}\mu_5^T=\frac{\partial\phi}{\partial x}+\frac{\mu_2^T}{\mu_1^T}\int_0^L e^{-\frac{|x-\bar{x}|}{k}}\frac{\partial\phi}{\partial\bar{x}}d\bar{x}$$
$$\frac{Q^T}{\eta_1}-\frac{\eta_3}{\eta_1}\frac{\partial^2\gamma_{xz}}{\partial x^2}-\frac{\eta_4}{\eta_1}\eta_5=\gamma_{xz}+\frac{\eta_2}{\eta_1}\int_0^L e^{-\frac{|x-\bar{x}|}{k}}\gamma_{xz}d\bar{x}. \tag{30}$$

Now, according to the transformation procedure presented in Eq. (2) and Eq. (3), the equal differential form of Eq. (30) can be obtained as follows:

$$M^T=EI\left(\zeta_1+\frac{(1-\zeta_1)l_m^2}{k^2}\right)\frac{\partial\phi}{\partial x}+ \frac{EI}{2k}\left(1-\frac{l_m^2}{k^2}\right)(1-\zeta_1)\int_0^L e^{-\frac{|x-\bar{x}|}{k}}\frac{\partial\phi}{\partial\bar{x}}d\bar{x}-\zeta_1EIl_m^2\frac{\partial^3\phi}{\partial x^3} -\frac{(1-\zeta_1)}{2k^2}EI\,l_m^2\left(St_1^Te^{-\frac{x}{k}}+St_2^Te^{\frac{x-L}{k}}\right)$$
$$Q^T=K_sGA\left(\zeta_1+\frac{(1-\zeta_1)l_m^2}{k^2}\right)\gamma_{xz}+ \frac{K_sGA}{2k}\left(1-\frac{l_m^2}{k^2}\right)(1-\zeta_1)\int_0^L e^{-\frac{|x-\bar{x}|}{k}}\left(\frac{\partial w^T}{\partial\bar{x}}+\phi\right)d\bar{x}-\zeta_1K_sGAl_m^2\left(\frac{\partial^3w^T}{\partial x^3}+\frac{\partial^2\phi}{\partial x^2}\right) -\frac{(1-\zeta_1)}{2k^2}K_sGA\,l_m^2\left(St_3^Te^{-\frac{x}{k}}+St_4^Te^{\frac{x-L}{k}}\right). \tag{28}$$

Here, to facilitate, the following symbols are introduced:

$$\frac{1}{\mu_1^T}\frac{\partial^2M^T}{\partial x^2}-\frac{\mu_3^T}{\mu_1^T}\frac{\partial^5\phi}{\partial x^5}-\frac{1}{k^2}\left[\frac{M^T}{\mu_1^T}-\frac{\mu_3^T}{\mu_1^T}\frac{\partial^3\phi}{\partial x^3}\right]=\frac{\partial^3\phi}{\partial x^3}-\frac{1}{k}\left(\frac{2\mu_2^T}{\mu_1^T}+\frac{1}{k}\right)\frac{\partial\phi}{\partial x}$$
$$\frac{1}{\eta_1}\frac{\partial^2Q^T}{\partial x^2}-\frac{\eta_3}{\eta_1}\frac{\partial^4\gamma_{xz}}{\partial x^4}-\frac{1}{k^2}\left[\frac{Q^T}{\eta_1}-\frac{\eta_3}{\eta_1}\frac{\partial^2\gamma_{xz}}{\partial x^2}\right]=\frac{\partial^2\gamma_{xz}}{\partial x^2}-\frac{1}{k}\left(\frac{2\eta_2}{\eta_1}+\frac{1}{k}\right)\gamma_{xz}. \tag{31}$$

Also, the essential CBCs should be derived using Eq. (4). Therefore:

into Eq. (33). These equations are written as follows by applying the symbols introduced in Eq. (29):

$$\frac{1}{\mu_1^T}\frac{\partial M^T}{\partial x}-\frac{\mu_3^T}{\mu_1^T}\frac{\partial^4\phi}{\partial x^4}-\frac{\mu_4^T}{\mu_1^T}\frac{\partial\mu_5^T}{\partial x}-\frac{1}{k}\left[\frac{M^T}{\mu_1^T}-\frac{\mu_3^T}{\mu_1^T}\frac{\partial^3\phi}{\partial x^3}-\frac{\mu_4^T}{\mu_1^T}\mu_5^T\right]=\frac{\partial^2\phi}{\partial x^2}-\frac{1}{k}\frac{\partial\phi}{\partial x}\ at\,x=0$$
$$\frac{1}{\mu_1^T}\frac{\partial M^T}{\partial x}-\frac{\mu_3^T}{\mu_1^T}\frac{\partial^4\phi}{\partial x^4}-\frac{\mu_4^T}{\mu_1^T}\frac{\partial\mu_5^T}{\partial x}+\frac{1}{k}\left[\frac{M^T}{\mu_1^T}-\frac{\mu_3^T}{\mu_1^T}\frac{\partial^3\phi}{\partial x^3}-\frac{\mu_4^T}{\mu_1^T}\mu_5^T\right]=\frac{\partial^2\phi}{\partial x^2}+\frac{1}{k}\frac{\partial\phi}{\partial x}\ at\,x=L \tag{32}$$

$$\frac{1}{\eta_1}\frac{\partial Q^T}{\partial x}-\frac{\eta_3}{\eta_1}\frac{\partial^3\gamma_{xz}}{\partial x^3}-\frac{\eta_4}{\eta_1}\frac{\partial\eta_5}{\partial x}-\frac{1}{k}\left[\frac{Q^T}{\eta_1}-\frac{\eta_3}{\eta_1}\frac{\partial^2\gamma_{xz}}{\partial x^2}-\frac{\eta_4}{\eta_1}\eta_5\right]=\frac{\partial\gamma_{xz}}{\partial x}-\frac{1}{k}\gamma_{xz}\ at\,x=0$$
$$\frac{1}{\eta_1}\frac{\partial Q^T}{\partial x}-\frac{\eta_3}{\eta_1}\frac{\partial^3\gamma_{xz}}{\partial x^3}-\frac{\eta_4}{\eta_1}\frac{\partial\eta_5}{\partial x}+\frac{1}{k}\left[\frac{Q^T}{\eta_1}-\frac{\eta_3}{\eta_1}\frac{\partial^2\gamma_{xz}}{\partial x^2}-\frac{\eta_4}{\eta_1}\eta_5\right]=\frac{\partial\gamma_{xz}}{\partial x}+\frac{1}{k}\gamma_{xz}\ at\,x=L.$$

Now, the equilibrium equations associated with the TBT are written:

$$\frac{\partial Q^T}{\partial x}-m_1\frac{\partial^2 w^T}{\partial t^2}=0$$
$$\frac{\partial M^T}{\partial x}-Q^T-m_2\frac{\partial^2\phi}{\partial t^2}=0 \tag{33}$$
$$m_1=\rho A,\ m_2=\rho I.$$

In this step, by performing some mathematical manipulations on Eq. (33) to extract the second derivate of M^T and Q^T, and substituting them into Eq. (31), the LNSG bending moment as well as the LNSG shear force of TBT can be achieved in differential form:

$$M^T=-k^2\mu_3^T\frac{\partial^5\phi}{\partial x^5}+\left(\mu_3^T-k^2\mu_1^T\right)\frac{\partial^3\phi}{\partial x^3}$$
$$+\left(2\mu_2^Tk+\mu_1^T\right)\frac{\partial\phi}{\partial x}+k^2\left(m_2\frac{\partial^3\phi}{\partial t^2\partial x}+m_1\frac{\partial^2 w^T}{\partial t^2}\right)$$

$$Q^T=-k^2\eta_3\left(\frac{\partial^5 w^T}{\partial x^5}+\frac{\partial^4\phi}{\partial x^4}\right)+\left(\eta_3-k^2\eta_1\right)\left(\frac{\partial^3 w^T}{\partial x^3}+\frac{\partial^2\phi}{\partial x^2}\right)$$
$$+\left(2\eta_2k+\eta_1\right)\left(\frac{\partial w^T}{\partial x}+\phi\right)+k^2m_1\frac{\partial^3 w^T}{\partial t^2\partial x}. \tag{34}$$

Now, it is possible to extract the LNSG governing equations of Timoshenko nanobeams by substituting Eq. (34) into Eq. (33). These equations are written as follows by applying the symbols introduced in Eq. (29):

$$-m_1\frac{\partial^2 w^T}{\partial t^2}+K_sGA\frac{\partial\phi}{\partial x}+K_sGA\frac{\partial^2 w^T}{\partial x^2}+k^2m_1\frac{\partial^4 w^T}{\partial t^2\partial x^2}$$
$$-\left(K_sGAl_m^2+K_sGA\zeta_1k^2\right)\left(\frac{\partial^4 w^T}{\partial x^4}+\frac{\partial^3\phi}{\partial x^3}\right)$$
$$+K_sGAl_m^2\zeta_1k^2\left(\frac{\partial^6 w^T}{\partial x^6}+\frac{\partial^5\phi}{\partial x^5}\right)=0$$

$$K_sGA\left(\left(l_m^2+\zeta_1k^2\right)\frac{\partial^3 w^T}{\partial x^3}-\frac{\partial w^T}{\partial x}-l_m^2\zeta_1k^2\frac{\partial^5 w^T}{\partial x^5}\right)-m_2\frac{\partial^2\phi}{\partial t^2}-K_sGA\phi$$
$$+\left(EI+K_sGA\left(l_m^2+\zeta_1k^2\right)\right)\frac{\partial^2\phi}{\partial x^2}+k^2m_2\frac{\partial^4\phi}{\partial t^2\partial x^2}$$
$$-\left(K_sGAl_m^2\zeta_1k^2+EI\left(l_m^2+\zeta_1k^2\right)\right)\frac{\partial^4\phi}{\partial x^4}+EIk^2l_m^2\zeta_1\frac{\partial^6\phi}{\partial x^6}=0. \tag{35}$$

Similarly, the CBCs should be obtained in terms of w^T and ϕ by replacing the Eq. (34) into Eq. (32):

2.4 Exact solution

To achieve the exact solution of the Eq. (19), which is related to the EBT, as well as the solution of the governing equations corresponding to the TBT, i.e., Eq. (35), the separation of variables method is employed and non-dimensional parameters are introduced as follows:

$$w^E(x,t)=W^E(x)e^{i\omega t}\ \ for\,EBT$$

$$\begin{cases} w^T(x,t)=W^T(x)e^{i\omega t} \\ \phi(x,t)=\Phi(x)e^{i\omega t}\end{cases}\ for\,TBT$$

$$\bar{x}=\frac{x}{L},\ \overline{W}_E=\frac{W^E}{L}\ \overline{W}_T=\frac{W^T}{L}$$
$$\Gamma_1=\frac{k}{L},\ \Gamma_2=\frac{m_1L^2}{m_2},\ \Gamma_3=\frac{EI}{K_sGAL^2},\ \Gamma_4=\frac{l_m}{L},\ \lambda=\omega L^2\sqrt{\frac{m_1}{EI}}, \tag{36}$$

where ω and λ show the dimensional and non-dimensional vibration frequencies, respectively.

$$\lambda^2 - \Gamma_1^2\lambda^2 D^2 - D^4 + \left(\Gamma_4^2 + \Gamma_1^2\zeta_1\right)D^6 - \Gamma_1^2\Gamma_4^2\zeta_1 D^8 = 0. \quad (41)$$

Here, according to the higher order boundary conditions associated with the strain gradient, i.e., $\sigma_{xx}^{E1}\delta\varepsilon_{xx}^{E}\big|_0^L = 0$, the following boundary conditions must be satisfied:

$$\begin{aligned}
&\partial_{\bar{x},\bar{x}}\overline{W}_E = 0 \; or \; \sigma_{xx}^1 = 0 \to \zeta_1\partial_{\bar{x},\bar{x},\bar{x}}\overline{W}_E + \frac{(1-\zeta_1)}{2\Gamma_1}\int_0^1 e^{-\frac{y}{\Gamma_1}}\partial_{y,y,y}\overline{W}_E\,\mathrm{d}y = 0 \; at\,\bar{x} = 0\\
&\partial_{\bar{x},\bar{x}}\overline{W}_E = 0 \; or \; \sigma_{xx}^1 = 0 \to \zeta_1\partial_{\bar{x},\bar{x},\bar{x}}\overline{W}_E + \frac{(1-\zeta_1)}{2\Gamma_1}\int_0^1 e^{-\frac{1-y}{\Gamma_1}}\partial_{y,y,y}\overline{W}_E\,\mathrm{d}y = 0 \; at\,\bar{x} = 1.
\end{aligned} \quad (42)$$

2.4.1 EBT

In the first step, Eq. (19) is rewritten in the non-dimensional form:

$$\lambda^2\overline{W}_E - \overline{W}_E^{(4)} + \Gamma_4^2\overline{W}_E^{(6)} - \Gamma_1^2\left(\lambda^2\overline{W}_E'' - \zeta_1\overline{W}_E^{(6)} + \zeta_1\Gamma_4^2\overline{W}_E^{(8)}\right) = 0. \quad (37)$$

Next, the non-dimensional bending moment and shear force as well as two CBCs related to the EBT should be presented. Therefore:

$$\begin{aligned}
\overline{M}_E &= -\overline{W}_E'' + \Gamma_4^2\overline{W}_E^{(4)} - \Gamma_1^2\left(\lambda^2\overline{W}_E - \zeta_1\overline{W}_E^{(4)} + \zeta_1\Gamma_4^2\overline{W}_E^{(6)}\right)\\
\overline{Q}_E &= -\overline{W}_E^{(3)} + \Gamma_4^2\overline{W}_E^{(5)} - \Gamma_1^2\left(\lambda^2\overline{W}_E' - \zeta_1\overline{W}_E^{(6)} + \zeta_1\Gamma_4^2\overline{W}_E^{(7)}\right)
\end{aligned} \quad (38)$$

Finally, the vibration frequencies of the LNSG Euler–Bernoulli nanobeams can be obtained by constructing the constant coefficients matrix and find the values of λ which lead to zero determinant. It is helpful to be mentioned that there are eight boundary conditions including four geometrical or natural, two CBCs, Eq. (39), and two boundary conditions due to the strain gradient, Eq. (42).

2.4.2 TBT

The non-dimensional governing equations of TBT, Eq. (35), are rewritten as follows:

$$\begin{aligned}
&\left(\begin{array}{l}
(\zeta_1 - 1)\Gamma_4^2\overline{W}_E'' - (\zeta_1 - 1)\Gamma_1\Gamma_4^2\overline{W}_E^{(3)} - (\zeta_1 - 1)\Gamma_1^2\left(\overline{W}_E'' - \Gamma_4^2\overline{W}_E^{(4)}\right)\\
+(\zeta_1 - 1)\Gamma_1^3\left(\overline{W}_E^{(3)} - \Gamma_4^2\overline{W}_E^{(5)}\right) + \Gamma_1^4\left(\lambda^2\overline{W}_E - \zeta_1\overline{W}_E^{(4)} + \zeta_1\Gamma_4^2\overline{W}_E^{(6)}\right)\\
-\Gamma_1^5\left(\lambda^2\overline{W}_E' - \zeta_1\overline{W}_E^{(5)} + \zeta_1\Gamma_4^2\overline{W}_E^{(7)}\right) - \overline{W}_E''\left(-\Gamma_4^2 + \zeta_1\Gamma_4^2\right)
\end{array}\right) = 0 \;\; at\,\bar{x} = 0\\
&\left(\begin{array}{l}
(\zeta_1 - 1)\Gamma_4^2\overline{W}_E'' + (\zeta_1 - 1)\Gamma_1\Gamma_4^2\overline{W}_E^{(3)} - (\zeta_1 - 1)\Gamma_1^2\left(\overline{W}_E'' - \Gamma_4^2\overline{W}_E^{(4)}\right)\\
-(\zeta_1 - 1)\Gamma_1^3\left(\overline{W}_E^{(3)} - \Gamma_4^2\overline{W}_E^{(5)}\right) + \Gamma_1^4\left(\lambda^2\overline{W}_E - \zeta_1\overline{W}_E^{(4)} + \zeta_1\Gamma_4^2\overline{W}_E^{(6)}\right)\\
+\Gamma_1^5\left(\lambda^2\overline{W}_E' - \zeta_1\overline{W}_E^{(5)} + \zeta_1\Gamma_4^2\overline{W}_E^{(7)}\right) + \overline{W}_E''\left(\Gamma_4^2 - \zeta_1\Gamma_4^2\right)
\end{array}\right) = 0 \;\; at\,\bar{x} = 1.
\end{aligned} \quad (39)$$

Now, the general solution of Eq. (37), which is an eight-order differential equation with constant coefficients, can be considered as follows:

$$\overline{W}_E(\bar{x}) = \sum_{i=1}^{8} C_i e^{R_i\bar{x}}, \quad (40)$$

where R_i are the roots of the following equation and C_i are unknown coefficients which can be extracted by satisfying all boundary conditions:

$$\begin{aligned}
&\Phi' + \overline{W}_T'' + \lambda^2\Gamma_3\left(\overline{W}_T - \Gamma_1^2\overline{W}_T''\right) -\\
&\left(\zeta_1\Gamma_1^2 + \Gamma_4^2\right)\left(\Phi^{(3)} + \overline{W}_T^{(4)}\right) + \zeta_1\Gamma_1^2\Gamma_4^2\left(\Phi^{(5)} + \overline{W}_T^{(6)}\right) = 0\\[6pt]
&\frac{1}{\Gamma_2}\left(\begin{array}{l}
\lambda^2\Gamma_3\left(-\Phi + \Gamma_1^2\Phi''\right) +\\
\Gamma_2\left(\Phi + \overline{W}_T' - \left(\zeta_1\Gamma_1^2 + \Gamma_3 + \Gamma_4^2\right)\Phi'' - \left(\zeta_1\Gamma_1^2 + \Gamma_4^2\right)\overline{W}_T^{(3)}\right)
\end{array}\right) +\\
&\left(\begin{array}{l}
\left(\zeta_1\Gamma_1^2\Gamma_3 + \zeta_1\Gamma_1^2\Gamma_4^2 + \Gamma_3\Gamma_4^2\right)\Phi^{(4)}\\
+\zeta_1\Gamma_1^2\Gamma_4^2\overline{W}_T^{(5)} - \zeta_1\Gamma_1^2\Gamma_3\Gamma_4^2\Phi^{(6)}
\end{array}\right) = 0.
\end{aligned} \quad (43)$$

In addition, the LNSG bending moment and shear force should be represented in dimensionless form:

$$\overline{M} = \left(\Phi' - \Gamma_4^2\phi^{(3)}\right) - \frac{\Gamma_1^2}{\Gamma_2}\left(\lambda^2\Phi' + \Gamma_2\left(\lambda^2\overline{W}_T + \zeta_1\Phi^{(3)} - \zeta_1\Gamma_4^2\Phi^{(5)}\right)\right)$$

$$\begin{aligned}\overline{Q} = \Phi + \left(1 - \lambda^2\Gamma_1^2\Gamma_3\right)\overline{W}_T' - \left(\zeta_1\Gamma_1^2 + \Gamma_4^2\right)\Phi'' - \left(\zeta_1\Gamma_1^2 - \Gamma_4^2\right)\overline{W}_T^{(3)} \\ + \zeta_1\Gamma_1^2\Gamma_4^2\Phi^{(4)} + \zeta_1\Gamma_1^2\Gamma_4^2\overline{W}_T^{(5)}.\end{aligned} \tag{44}$$

Similarly, the non-dimensional form of all CBCs is obtained and pretend in Appendix. Afterward, using the derivative operator as $D^n \equiv \partial^n/\partial x^n$, the matrix form of Eq. (43) is presented:

$$\begin{bmatrix} \begin{array}{l}\zeta_1\Gamma_1^2\Gamma_4^2D^6 - \left(\zeta_1\Gamma_1^2 + \Gamma_4^2\right)D^4 \\ +\left(1 - \lambda^2\Gamma_1^2\Gamma_3\right)D^2 + \lambda^2\Gamma_3\end{array} & \zeta_1\Gamma_1^2\Gamma_4^2D^5 + \left(-\zeta_1\Gamma_1^2 - \Gamma_4^2\right)D^3 + D \\ \zeta_1\Gamma_1^2\Gamma_4^2D^5 + \left(-\zeta_1\Gamma_1^2 - \Gamma_4^2\right)D^3 + D & \begin{array}{c} -\zeta_1\Gamma_1^2\Gamma_3\Gamma_4^2D^6 + \\ \left(\zeta_1\Gamma_1^2\Gamma_3 + \zeta_1\Gamma_1^2\Gamma_4^2 + \Gamma_3\Gamma_4^2\right)D^4 + \\ \dfrac{\left(-\zeta_1\Gamma_1^2\Gamma_2 + \lambda^2\Gamma_1^2\Gamma_3 - \Gamma_2\Gamma_3 - \Gamma_2\Gamma_4^2\right)}{\Gamma_2}D^2 \\ +\dfrac{\Gamma_2 - \lambda^2\Gamma_3}{\Gamma_2}\end{array} \end{bmatrix} \begin{Bmatrix} \overline{W}_T \\ \Phi \end{Bmatrix} = 0. \tag{45}$$

Now, taking the determinant of the coefficients matrix of Eq. (45) gives:

$$\begin{aligned}&\left(-\zeta_1^2\Gamma_1^4\Gamma_3\Gamma_4^4\right)D^{12} + \left(2\zeta_1\Gamma_1^2\Gamma_3\Gamma_4^2\left(\zeta_1\Gamma_1^2 + \Gamma_4^2\right)\right)D^{10} + \\ &\frac{\Gamma_3}{\Gamma_2}\left(-4\zeta_1\Gamma_1^2\Gamma_2\Gamma_4^2 - \Gamma_2\Gamma_4^4 + \zeta_1\Gamma_1^4\left(\lambda^2\Gamma_4^2 + \Gamma_2\left(-\zeta_1 + \lambda^2\Gamma_3\Gamma_4^2\right)\right)\right)D^8 \\ &-\frac{\Gamma_3}{\Gamma_2}\begin{pmatrix} -2\Gamma_2\Gamma_4^2 + \zeta_1\lambda^2\Gamma_1^4\left(1 + \Gamma_2\left(\Gamma_3 + \Gamma_4^2\right)\right) + \\ \Gamma_1^2\left(\left(1 + \zeta_1\right)\lambda^2\Gamma_4^2 + \Gamma_2\left(-2\zeta_1 + \left(1 + \zeta_1\right)\lambda^2\Gamma_3\Gamma_4^2\right)\right)\end{pmatrix}D^6 + \\ &\frac{\Gamma_3}{\Gamma_2}\begin{pmatrix} \Gamma_1^4\left(\zeta_1\lambda^2\Gamma_2 - \lambda^4\Gamma_3\right) + \lambda^2\Gamma_4^2 + \Gamma_2\left(-1 + \lambda^2\Gamma_3\Gamma_4^2\right) + \\ \left(1 + \zeta_1\right)\lambda^2\Gamma_1^2\left(1 + \Gamma_2\left(\Gamma_3 + \Gamma_4^2\right)\right)\end{pmatrix}D^4 + \\ &\frac{\lambda^2\Gamma_3}{\Gamma_2}\left(-1 - \Gamma_1^2\left(\left(1 + \zeta_1\right)\Gamma_2 - 2\lambda^2\Gamma_3\right) - \Gamma_2\left(\Gamma_3 + \Gamma_4^2\right)\right)D^2 + \\ &\lambda^2\Gamma_3\left(1 - \frac{\lambda^2\Gamma_3}{\Gamma_2}\right) = 0.\end{aligned} \tag{46}$$

It is worth noting that, as can be seen from Eq. (46), the order of corresponding governing differential equation of LNSG Timoshenko nanobeam is 12 which is equal to the total number of boundary conditions including 4 natural or geometric BCs, 4 BCs related to the strain gradient, and 4 CBCs relevant to the transformation of integral equations to differential ones. Accordingly, the exact solution of Eq. (43) can be obtained by satisfying all boundary conditions. Therefore, the general solution of this differential equation is considered as follows:

$$\begin{aligned}\overline{W}_T(\overline{x}) &= \sum_{i=1}^{12} C_i e^{R_i\overline{x}} \\ \Phi(\overline{x}) &= \sum_{i=1}^{12} \alpha_i C_i e^{R_i\overline{x}},\end{aligned} \tag{47}$$

in which C_i are constant coefficients, R_i are the roots of Eq. (46) and:

$$\alpha_i = \frac{-\lambda^2\Gamma_3 + R_i^2\left(-1 + \lambda^2\Gamma_1^2\Gamma_3\right) - \zeta_1R_i^6\Gamma_1^2\Gamma_4^2 + R_i^4\left(\zeta_1\Gamma_1^2 + \Gamma_4^2\right)}{R_i\left(-1 + \zeta_1R_i^2\Gamma_1^2\right)\left(-1 + R_i^2\Gamma_4^2\right)}. \tag{48}$$

As previously mentioned and also, it can be seen from the Eq. (23), the higher order boundary conditions related to the strain gradient, i.e., $\sigma_{kl}^1\delta\varepsilon_{kl}\Big|_0^L = 0$, must be satisfied. Owing this, it is essential to be considered that:

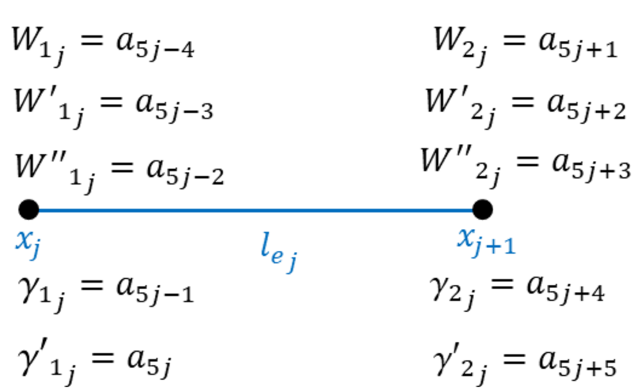

Fig. 2 Two-node beam element with five degrees of freedom per node

$$\begin{aligned}
&\partial_{\bar{x}}\Phi = 0 \; or \; \sigma_{xx}^{1} = 0 \rightarrow \zeta_1 \partial_{\bar{x},\bar{x}}\Phi + \frac{(1-\zeta_1)}{2\Gamma_1}\int_0^1 e^{-\frac{y}{\Gamma_1}}\partial_{y,y}\Phi \, \mathrm{d}y = 0 \; at \; \bar{x} = 0 \\
&\partial_{\bar{x}}\Phi = 0 \; or \; \sigma_{xx}^{1} = 0 \rightarrow \zeta_1 \partial_{\bar{x},\bar{x}}\Phi + \frac{(1-\zeta_1)}{2\Gamma_1}\int_0^1 e^{-\frac{1-y}{\Gamma_1}}\partial_{y,y}\Phi \, \mathrm{d}y = 0 \; at \; \bar{x} = 1 \\
&\Phi + \partial_{\bar{x}}\overline{W}_T = 0 \; or \; \sigma_{xz}^{1} = 0 \rightarrow \zeta_1\left(\partial_{\bar{x}}\Phi + \partial_{\bar{x},\bar{x}}\overline{W}_T\right) + \frac{(1-\zeta_1)}{2\Gamma_1}\int_0^1 e^{-\frac{y}{\Gamma_1}}\left(\partial_y\Phi + \partial_{y,y}\overline{W}_T\right)\mathrm{d}y = 0 \; at \; \bar{x} = 0 \\
&\Phi + \partial_{\bar{x}}\overline{W}_T = 0 \; or \; \sigma_{xz}^{1} = 0 \rightarrow \zeta_1\left(\partial_{\bar{x}}\Phi + \partial_{\bar{x},\bar{x}}\overline{W}_T\right) + \frac{(1-\zeta_1)}{2\Gamma_1}\int_0^1 e^{-\frac{1-y}{\Gamma_1}}\left(\partial_y\Phi + \partial_{y,y}\overline{W}_T\right)\mathrm{d}y = 0 \; at \; \bar{x} = 1.
\end{aligned} \tag{49}$$

Now, by satisfying all 12 BCs, the coefficients matrix is constructed, and then, its determinant should be set equal to zero for extracting the characteristic equation.

Finally, the vibration frequencies of LNSG Timoshenko beams are obtained by solving this equation by employing numerical ways such as the method presented in Reference [66]. It is helpful to note that to prevent ill-conditioning, all elements of each column of the coefficients matrix are divided by the norm of that column.

2.5 Local/nonlocal strain gradient finite-element model

First of all, it should be noted that the present FEM of LNSG is constructed using the basic integral form of the LNSG Timoshenko beam and no transformation is implemented on the integral equation. Also, to create an efficient shear-locking-free beam element, the shear strain is considered as an independent degree of freedom and the order of element is set in such a way that the derivative of the strains related to the strain gradient is not neglected. Therefore, the rotation of cross section is rewritten as follows by this assumption that $\gamma = -\gamma_{xy}$:

$$\phi(x,t) = -\left(\frac{\partial w}{\partial x} + \gamma\right). \tag{50}$$

Now, according to Eq. (21), Eq. (22), and Eq. (50), the strain potential energy, per length, of the LNSG Timoshenko nanobeam can be expressed:

$$\begin{aligned}
&\overline{U} = \frac{1}{2}\int_A \left[\sigma_{xx}^{T}\varepsilon_{xx}^{T} + \sigma_{xx}^{T1}\varepsilon_{xx,x}^{T} + \sigma_{xz}\gamma_{xz} + \sigma_{xz}^{1}\gamma_{xz,x}\right]dA \\
&\overline{U} = \zeta_1\overline{U}^{L} + \left(1-\zeta_1\right)\overline{U}^{NL} \\
&\alpha = EI, \;\; \beta = K_s GA \\
&\overline{U}^{L} = \frac{\alpha}{2}\left[\left(\frac{\partial\gamma}{\partial x} + \frac{\partial^2 w}{\partial x^2}\right)^2 + l_m^2\left(\frac{\partial^2\gamma}{\partial x^2} + \frac{\partial^3 w}{\partial x^3}\right)^2\right] + \frac{\beta}{2}\left(\gamma^2 + l_m^2\left(\frac{\partial\gamma}{\partial x}\right)^2\right) \\
&\overline{U}^{NL} = \frac{\alpha}{4k}\left[\int_0^L e^{-\frac{|x-\bar{x}|}{k}}\left(\frac{\partial\gamma}{\partial\bar{x}} + \frac{\partial^2 w}{\partial\bar{x}^2}\right)d\bar{x}\right]\left(\frac{\partial\gamma}{\partial x} + \frac{\partial^2 w}{\partial x^2}\right) \\
&+\frac{\alpha}{4k}\left[\int_0^L e^{-\frac{|x-\bar{x}|}{k}} l_m^2\left(\frac{\partial^2\gamma}{\partial\bar{x}^2} + \frac{\partial^3 w}{\partial\bar{x}^3}\right)d\bar{x}\right]\left(\frac{\partial^2\gamma}{\partial x^2} + \frac{\partial^3 w}{\partial x^3}\right) \\
&+\frac{\beta}{4k}\left(\int_0^L e^{-\frac{|x-\bar{x}|}{k}}\gamma\left(\bar{x}\right)d\bar{x}\right)\gamma(x) \\
&+\frac{\beta}{4k}\left(\int_0^L e^{-\frac{|x-\bar{x}|}{k}} l_m^2\frac{\partial\gamma}{\partial\bar{x}}d\bar{x}\right)\frac{\partial\gamma}{\partial x}.
\end{aligned} \tag{51}$$

In which the superscripts "L" and "NL" stand for the local and nonlocal cases, respectively. Now, a two-node beam element with five degrees of freedom per node is introduced as Fig. 2 for jth element. In fact, to consider the influences of strain gradient, the higher order form of the beam element proposed in Reference [43] is considered.

Due to independency of the shear strain from the transverse displacement, the shape functions of them can be easily derived as follow. These shape functions are presented as functions of x which is the axial distance from the beginning of the beam:

$$
\begin{aligned}
w_j(x) &= \sum_{n=5j-4}^{5j+5} N_n^w a_n \\
\gamma_j(x) &= \sum_{n=5j-4}^{5j+5} N_n^\gamma a_n,
\end{aligned}
\tag{53}
$$

where a_n are the degrees of freedom that are illustrated in Fig. 2. In this step, the nonlocal strain gradient potential energy of the jth element which is resulted from the contribution of the ith element is written as Eq. (54):

$$
\begin{aligned}
&\left\{N^w_{5j-4}, N^w_{5j-3}, N^w_{5j-2}, N^w_{5j-1}, N^w_{5j}, N^w_{5j+1}, N^w_{5j+2}, N^w_{5j+3}, N^w_{5j+4}, N^w_{5j+5}\right\} = \\
&\left\{\begin{array}{l}
-\dfrac{\left(l_{e_j}^2 + 3l_{e_j}(x-x_j) + 6(x-x_j)^2\right)\left(x - l_{e_j} - x_j\right)^3}{l_{e_j}^5}, \\
-\dfrac{\left(l_{e_j} + 3\left(x-x_j\right)\right)\left(x-x_j\right)\left(x - l_{e_j} - x_j\right)^3}{l_{e_j}^4}, \\
-\dfrac{\left(x-x_j\right)^2\left(x - l_{e_j} - x_j\right)^3}{2l_{e_j}^3}, 0, 0, \\
\dfrac{\left(10l_{e_j}^2 - 15l_{e_j}(x-x_j) + 6(x-x_j)^2\right)\left(x-x_j\right)^3}{l_{e_j}^5}, \\
\dfrac{\left(-4l_{e_j}^2 + 7l_{e_j}(x-x_j) - 3(x-x_j)^2\right)\left(x-x_j\right)^3}{l_{e_j}^4}, \\
\dfrac{(x-x_j)^3\left(x - l_{e_j} - x_j\right)^2}{2l_{e_j}^3}, 0, 0
\end{array}\right\} \\
&\left\{N^\gamma_{5j-4}, N^\gamma_{5j-3}, N^\gamma_{5j-2}, N^\gamma_{5j-1}, N^\gamma_{5j}, N^\gamma_{5j+1}, N^\gamma_{5j+2}, N^\gamma_{5j+3}, N^\gamma_{5j+4}, N^\gamma_{5j+5}\right\} = \\
&\left\{\begin{array}{l}
0, 0, 0, 1 - \dfrac{3(x-x_j)^2}{l_{e_j}^2} + \dfrac{2(x-x_j)^3}{l_{e_j}^3}, (x-x_j) - \dfrac{2(x-x_j)^2}{l_{e_j}} + \dfrac{(x-x_j)^3}{l_{e_j}^2} \\
0, 0, 0, \dfrac{3(x-x_j)^2}{l_{e_j}^2} - \dfrac{2(x-x_j)^3}{l_{e_j}^3}, -\dfrac{(x-x_j)^2}{l_{e_j}} + \dfrac{(x-x_j)^3}{l_{e_j}^2}
\end{array}\right\}
\end{aligned}
\tag{52}
$$

Now, for the jth element, it can be written as:

Table 1 The first four non-dimensional vibration frequencies of two-phase strain gradient SSSS nanobeams, $k/L=0.05$, $l_m/L=0.10$

	ζ_1		# Of element	1st	2nd	3rd	4th
$h/L=0.01$	0.10	FEM	10	10.1960	44.2310	109.8706	214.9033
			20	10.1958	44.2293	109.8646	214.8913
			30	10.1958	44.2292	109.8643	214.8906
			40	10.1958	44.2292	109.8642	214.8905
		Exact-TBT	–	10.1958	44.2292	109.8642	214.8904
		Exact-EBT	–	10.1972	44.2545	110.0107	215.4134
	0.50	FEM	10	10.2638	45.3203	115.4446	232.7452
			20	10.2638	45.3203	115.4444	232.7438
			30	10.2638	45.3203	115.4444	232.7438
			40	10.2638	45.3203	115.4444	232.7438
		Exact-TBT	–	10.2638	45.3203	115.4444	232.7438
		Exact-EBT	–	10.2651	45.3450	115.5936	233.2995
$h/L=0.20$	0.10	FEM	10	9.6875	37.0270	78.6826	131.1593
			20	9.6867	37.0194	78.6605	131.1256
			30	9.6867	37.0189	78.6591	131.1234
			40	9.6867	37.0188	78.6589	131.12308
		Exact-TBT	–	9.6867	37.0188	78.6588	131.1230
		Exact-EBT	–	10.1972	44.2545	110.0107	215.4134
	0.50	FEM	10	9.7821	38.1903	83.1985	141.9528
			20	9.7820	38.1900	83.1978	141.9511
			30	9.7820	38.1900	83.1978	141.9510
			40	9.7820	38.1900	83.1978	141.9510
		Exact-TBT	–	9.7820	38.1900	83.1978	141.9510
		Exact-EBT	–	10.2651	45.3450	115.5936	233.2995

$$
\begin{aligned}
U_{ji}^{NL} &= \frac{\alpha}{4k}\int_{x_j}^{x_{j+1}}\left[\int_{x_i}^{x_{i+1}} e^{-\frac{|x-\bar{x}|}{k}}\left(\frac{\partial \gamma_i}{\partial \bar{x}}+\frac{\partial^2 w_i}{\partial \bar{x}^2}\right)d\bar{x}\right]\left(\frac{\partial \gamma_j}{\partial x}+\frac{\partial^2 w_j}{\partial x^2}\right)dx\\
&+\frac{\alpha}{4k}\int_{x_j}^{x_{j+1}}\left[\int_{x_i}^{x_{i+1}} e^{-\frac{|x-\bar{x}|}{k}} l_m^2\left(\frac{\partial^2 \gamma_i}{\partial \bar{x}^2}+\frac{\partial^3 w_i}{\partial \bar{x}^3}\right)d\bar{x}\right]\left(\frac{\partial^2 \gamma_j}{\partial x^2}+\frac{\partial^3 w_j}{\partial x^3}\right)dx\\
&+\frac{\beta}{4k}\int_{x_j}^{x_{j+1}}\left(\int_{x_i}^{x_{i+1}} e^{-\frac{|x-\bar{x}|}{k}}\gamma_i(\bar{x})d\bar{x}\right)\gamma_j(x)dx\\
&+\frac{\beta}{4k}\int_{x_j}^{x_{j+1}}\left(\int_{x_i}^{x_{i+1}} e^{-\frac{|x-\bar{x}|}{k}} l_m^2\frac{\partial \gamma_i}{\partial \bar{x}}d\bar{x}\right)\frac{\partial \gamma_j}{\partial x}dx\\
\alpha &= EI,\ \ \beta = K_sGA.
\end{aligned}
\tag{54}
$$

As can be seen from Eq. (54), due to integral nonlocal stress, all elements are coupled with together. Given this, three different types of nonlocal strain gradient stiffness element are defined according to the location of jth element relative to the ith element position. Therefore:

Table 2 The first four non-dimensional vibration frequencies of two-phase strain gradient CSFS nanobeams, $k/L=0.05$, $l_m/L=0.10$

	ζ_1		# Of element	1st	2nd	3rd	4th
$h/L=0.01$	0.10	FEM	10	4.0095	26.1238	78.5879	167.5304
			20	4.0067	26.1029	78.5143	167.3487
			30	4.0066	26.1017	78.5101	167.3381
			40	4.0066	26.1015	78.5095	167.3368
		Exact-TBT	–	4.0066	26.1015	78.5093	167.3365
		Exact-EBT	–	4.0069	26.1177	78.6247	167.7862
	0.50	FEM	10	4.1760	27.4340	83.9691	183.4334
			20	4.1759	27.4331	83.9650	183.4209
			30	4.1759	27.4331	83.9649	183.4206
			40	4.1759	27.4331	83.9649	183.4206
		Exact-TBT	–	4.1759	27.4331	83.9649	183.4206
		Exact-EBT	–	4.1763	27.4507	84.0928	183.9324
$h/L=0.20$	0.10	FEM	10	3.8752	21.3879	54.2124	97.1308
			20	3.8726	21.3731	54.1731	97.0610
			30	3.8725	21.3723	54.1707	97.0567
			40	3.8725	21.3721	54.1704	97.0562
		Exact-TBT	–	3.8725	21.3721	54.1703	97.0560
		Exact-EBT	–	4.0069	26.1177	78.6247	167.7862
	0.50	FEM	10	4.0313	22.3207	57.3520	104.7240
			20	4.0312	22.3201	57.3501	104.7202
			30	4.0312	22.3200	57.3500	104.7201
			40	4.0312	22.3200	57.3500	104.7201
		Exact-TBT	–	4.0312	22.3200	57.3500	104.7201
		Exact-EBT	–	4.1763	27.4507	84.0928	183.9324

$$
\begin{aligned}
& for\, j > i \\
& m = 5i-4, 5i-3, ..., 5i+4, 5i+5 \\
& n = 5j-4, 5j-3, ..., 5j+4, 5j+5 \\
& knl_{mn}^{ij} = \int_{x_j}^{x_{j+1}} \left[\frac{\alpha}{2k} \int_{x_i}^{x_{i+1}} e^{-\frac{x-\bar{x}}{k}} \left(\frac{\partial^2 N_m^w}{\partial \bar{x}^2} + \frac{\partial N_m^\gamma}{\partial \bar{x}} \right) d\bar{x} \right] \left(\frac{\partial^2 N_n^w}{\partial x^2} + \frac{\partial N_n^\gamma}{\partial x} \right) dx \\
& + \int_{x_j}^{x_{j+1}} \left[\frac{\beta}{2k} \int_{x_i}^{x_{i+1}} e^{-\frac{x-\bar{x}}{k}} \left(N_m^\gamma \right) d\bar{x} \right] \left(N_n^\gamma \right) dx \\
& + \int_{x_j}^{x_{j+1}} \left[\frac{l_m^2 \alpha}{2k} \int_{x_i}^{x_{i+1}} e^{-\frac{x-\bar{x}}{k}} \left(\frac{\partial^3 N_m^w}{\partial \bar{x}^3} + \frac{\partial^2 N_m^\gamma}{\partial \bar{x}^2} \right) d\bar{x} \right] \left(\frac{\partial^3 N_n^w}{\partial x^3} + \frac{\partial^2 N_n^\gamma}{\partial x^2} \right) dx \\
& + \int_{x_j}^{x_{j+1}} \left[\frac{l_m^2 \beta}{2k} \int_{x_i}^{x_{i+1}} e^{-\frac{x-\bar{x}}{k}} \left(\frac{\partial N_m^\gamma}{\partial \bar{x}} \right) d\bar{x} \right] \left(\frac{\partial N_n^\gamma}{\partial x} \right) dx.
\end{aligned}
\tag{55}
$$

Table 3 The first four non-dimensional vibration frequencies of two-phase strain gradient CSCS nanobeams, $k/L = 0.05$, $l_m/L = 0.10$

	ζ_1		# Of element	1st	2nd	3rd	4th
$h/L = 0.01$	0.10	FEM	10	30.1902	88.4054	185.4841	327.2339
			20	30.1394	88.2344	185.0767	326.4289
			30	30.1365	88.2244	185.0531	326.3821
			40	30.1361	88.2232	185.0501	326.3763
		Exact-TBT	–	30.1360	88.2229	185.0494	326.3747
		Exact-EBT	–	30.1630	88.4021	185.6992	328.1158
	0.50	FEM	10	33.2106	98.9171	212.2762	384.6866
			20	33.2080	98.9069	212.2469	384.6108
			30	33.2080	98.9067	212.2462	384.6091
			40	33.2080	98.9066	212.2461	384.6090
		Exact-TBT	–	33.2080	98.9066	212.2461	384.6089
		Exact-EBT	–	33.2404	99.1259	213.0598	386.8484
$h/L = 0.20$	0.10	FEM	10	23.1542	55.1064	97.7910	148.8453
			20	23.1224	55.0300	97.6542	148.6507
			30	23.1205	55.0254	97.6457	148.6383
			40	23.1203	55.0248	97.6446	148.6366
		Exact-TBT	–	23.1202	55.0246	97.6443	148.6361
		Exact-EBT	–	30.1630	88.4021	185.6992	328.1158
	0.50	FEM	10	25.0153	60.0106	108.4558	167.8622
			20	25.0139	60.0068	108.4487	167.8521
			30	25.0138	60.0067	108.4485	167.8518
			40	25.0138	60.0066	108.4485	167.8518
		Exact-TBT	–	25.0138	60.0066	108.4485	167.8518
		Exact-EBT	–	33.2404	99.1259	213.0598	386.8484

Table 4 The first four non-dimensional frequencies of LNSG nanobeams with SFSF, CFFF, and CFCF boundary conditions. $h/L = 0.10$, $k/L = 0.05$, and $\zeta_1 = 0.10$

B.C	L_m/L		1st	2nd	3rd	4th
SFSF	0.01	FEM	9.59765	35.5311	71.4561	111.313
		Exact-TBT	9.59759	35.5302	71.4529	111.306
		Exact-EBT	9.77332	38.0160	81.9950	138.413
	0.10	FEM	9.87936	39.9565	91.9994	167.369
		Exact-TBT	9.87936	39.9565	91.9992	167.368
		Exact-EBT	10.0511	42.4512	103.612	201.864
CFFF	0.01	FEM	3.27844	19.4821	50.0303	87.4159
		Exact-TBT	3.27814	19.4799	50.0242	87.4047
		Exact-EBT	3.30270	20.4753	55.8353	105.131
	0.10	FEM	3.40853	22.2859	63.6034	125.342
		Exact-TBT	3.40852	22.2858	63.6029	125.340
		Exact-EBT	3.43523	23.6115	72.6312	156.761
CFCF	0.01	FEM	18.5304	46.7411	82.1336	120.081
		Exact-TBT	18.5265	46.7304	82.1145	120.053
		Exact-EBT	19.6305	52.9152	100.2635	158.850
	0.10	FEM	22.8086	64.5556	126.184	205.344
		Exact-TBT	22.8084	64.5546	126.181	205.339
		Exact-EBT	24.6365	77.0886	168.305	304.566

Table 5 Comparison between the first non-dimensional vibration frequency of the present LNSG Timoshenko nanobeams with $h=0.0001$ L and $l_m/L=0$ with those of two-phase Euler–Bernoulli nanobeams provided through the exact solution (exact) proposed in Reference[42]

B.C	k/L		ζ_1				
			0.05	0.10	0.50	0.75	1.00
SS	0.05	Present-FEM	9.76014	9.76715	9.81485	9.84255	9.86960
		Exact [42]	9.76014	9.76715	9.81485	9.84255	9.86960
	0.10	Present-FEM	9.46849	9.49880	9.67978	9.77714	9.86960
		Exact [42]	9.46849	9.49880	9.67978	9.77714	9.86960
CF	0.05	Present-FEM	3.26170	3.29081	3.41739	3.47050	3.51602
		Exact [42]	3.26167	3.29081	3.41739	3.47050	3.51602
	0.10	Present-FEM	3.04116	3.09381	3.32818	3.42887	3.51602
		Exact [42]	3.04116	3.09381	3.32818	3.42887	3.51602
CC	0.05	Present-FEM	19.0815	19.4233	21.0156	21.7345	22.3733
		Exact [42]	19.0812	19.4232	21.0156	21.7345	22.3733
	0.10	Present-FEM	16.3555	16.9236	19.7732	21.1379	22.3733
		Exact [42]	16.3555	16.9236	19.7732	21.1379	22.3733

Table 6 Comparison between the first two frequency ratios of the present LNSG Timoshenko nanobeams with $h=0.0001$ L, $l_m/L=0.20$, and $\zeta_1 \simeq 0.0$ with those of integral nonlocal strain gradient Euler–Bernoulli nanobeams [59]

B.C		0.01		0.05		0.1		0.2	
		1st	2nd	1st	2nd	1st	2nd	1st	2nd
SFSF	Present-FEM	1.06213	1.3095	1.04687	1.26033	1.0198	1.16396	0.94825	0.94479
	Reference [59]	1.06213	1.3095	1.04687	1.26032	1.01977	1.16391	0.94812	0.94465
SSSS	Present-FEM	1.1755	1.58848	1.14424	1.47448	1.09906	1.30472	1	1.00001
	Reference [59]	1.17551	1.58851	1.14403	1.47394	1.09896	1.30453	0.99999	0.99999
CFFF	Present-FEM	1.05518	1.35113	1.0233	1.30239	0.97719	1.20268	0.87883	0.97787
	Reference [59]	1.05518	1.35112	1.02327	1.30224	0.97708	1.20221	0.87855	0.97692
CSFS	Present-FEM	1.46868	1.71322	1.34245	1.5247	1.20901	1.31569	1.00661	1.00669
	Reference [59]	1.46868	1.71314	1.34054	1.5222	1.20717	1.31352	1.00506	1.00509
CFCF	Present-FEM	1.61653	2.14515	1.51902	1.93537	1.32977	1.55395	0.9729	1.00592
	Reference [59]	1.6165	2.14508	1.51862	1.93423	1.32867	1.55154	0.97119	1.00331
CSCS	Present-FEM	2.40579	2.81432	1.93993	2.19268	1.51347	1.62454	1.01343	1.01358
	Reference [59]	2.40561	2.81361	1.93373	2.18515	1.50852	1.61894	1.01024	1.01021

$$
\begin{aligned}
&For\, j = i\\
&m = 5i-4, 5i-3, \ldots, 5i+4, 5i+5\\
&n = 5i-4, 5i-3, \ldots, 5i+4, 5i+5\\
&knl^{ii}_{mn} = \int_{x_i}^{x_{i+1}} \left[\frac{\alpha}{2k}\left(\int_{x_i}^{x} e^{-\frac{x-\bar{x}}{k}}\left(\frac{\partial^2 N^w_m}{\partial \bar{x}^2}+\frac{\partial N^\gamma_m}{\partial \bar{x}}\right)d\bar{x}\right)\right]\left(\frac{\partial^2 N^w_n}{\partial x^2}+\frac{\partial N^\gamma_n}{\partial x}\right)dx\\
&+\int_{x_i}^{x_{i+1}} \left[\frac{\alpha}{2k}\left(\int_{x}^{x_{i+1}} e^{\frac{x-\bar{x}}{k}}\left(\frac{\partial^2 N^w_m}{\partial \bar{x}^2}+\frac{\partial N^\gamma_m}{\partial \bar{x}}\right)d\bar{x}\right)\right]\left(\frac{\partial^2 N^w_n}{\partial x^2}+\frac{\partial N^\gamma_n}{\partial x}\right)dx\\
&+\int_{x_i}^{x_{i+1}} \left[\frac{\beta}{2k}\left(\int_{x_i}^{x} e^{-\frac{x-\bar{x}}{k}}\left(N^\gamma_m\right)d\bar{x}+\int_{x}^{x_{i+1}} e^{\frac{x-\bar{x}}{k}}\left(N^\gamma_m\right)d\bar{x}+\right)\right]\left(N^\gamma_n\right)dx\\
&+\int_{x_i}^{x_{i+1}} \left[\frac{l_m^2\alpha}{2k}\left(\int_{x_i}^{x} e^{-\frac{x-\bar{x}}{k}}\left(\frac{\partial^3 N^w_m}{\partial \bar{x}^3}+\frac{\partial^2 N^\gamma_m}{\partial^2 \bar{x}}\right)d\bar{x}\right)\right]\left(\frac{\partial^3 N^w_n}{\partial x^3}+\frac{\partial^2 N^\gamma_n}{\partial x^2}\right)dx\\
&+\int_{x_i}^{x_{i+1}} \left[\frac{l_m^2\alpha}{2k}\left(\int_{x}^{x_{i+1}} e^{\frac{x-\bar{x}}{k}}\left(\frac{\partial^3 N^w_m}{\partial \bar{x}^3}+\frac{\partial^2 N^\gamma_m}{\partial \bar{x}^2}\right)d\bar{x}\right)\right]\left(\frac{\partial^3 N^w_n}{\partial x^3}+\frac{\partial^2 N^\gamma_n}{\partial x^2}\right)dx\\
&+\int_{x_i}^{x_{i+1}} \left[\frac{l_m^2\beta}{2k}\left(\int_{x_i}^{x} e^{-\frac{x-\bar{x}}{k}}\left(\frac{\partial N^\gamma_m}{\partial \bar{x}}\right)d\bar{x}+\int_{x}^{x_{i+1}} e^{\frac{x-\bar{x}}{k}}\left(\frac{\partial N^\gamma_m}{\partial \bar{x}}\right)d\bar{x}+\right)\right]\left(\frac{\partial N^\gamma_n}{\partial x}\right)dx.
\end{aligned}
\tag{56}
$$

Fig. 3 Influence of l_m/k on the fundamental frequency ratios of LNSG nanobeams with different boundary conditions and thickness ratios, $\zeta_1 = 0.01$, $k/L = 0.10$

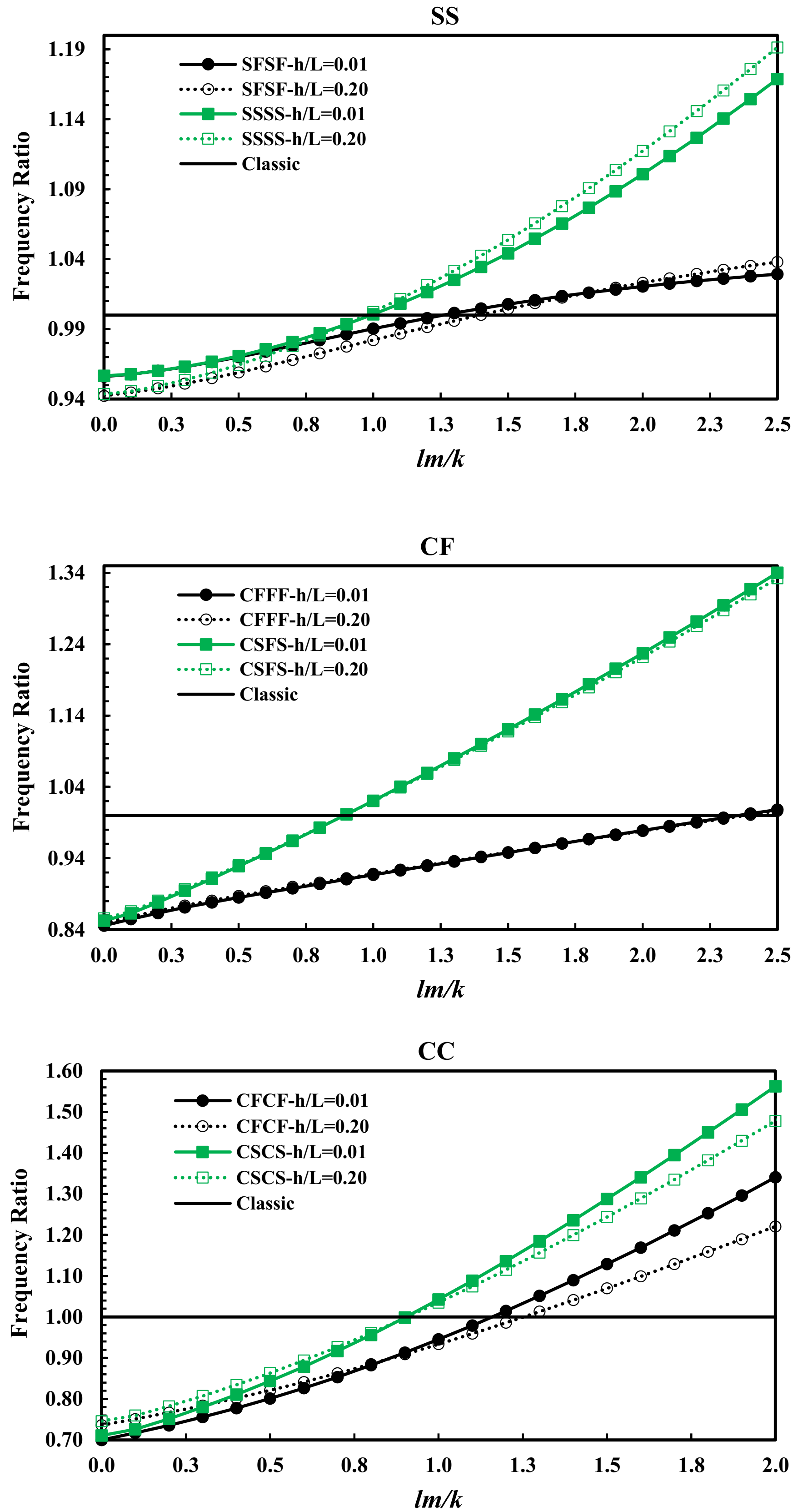

Figure. 4 Influence of local phase fraction factor on the fundamental frequency ratios of LNSG nanobeams with different boundary conditions, $h/L = k/L = 0.10$

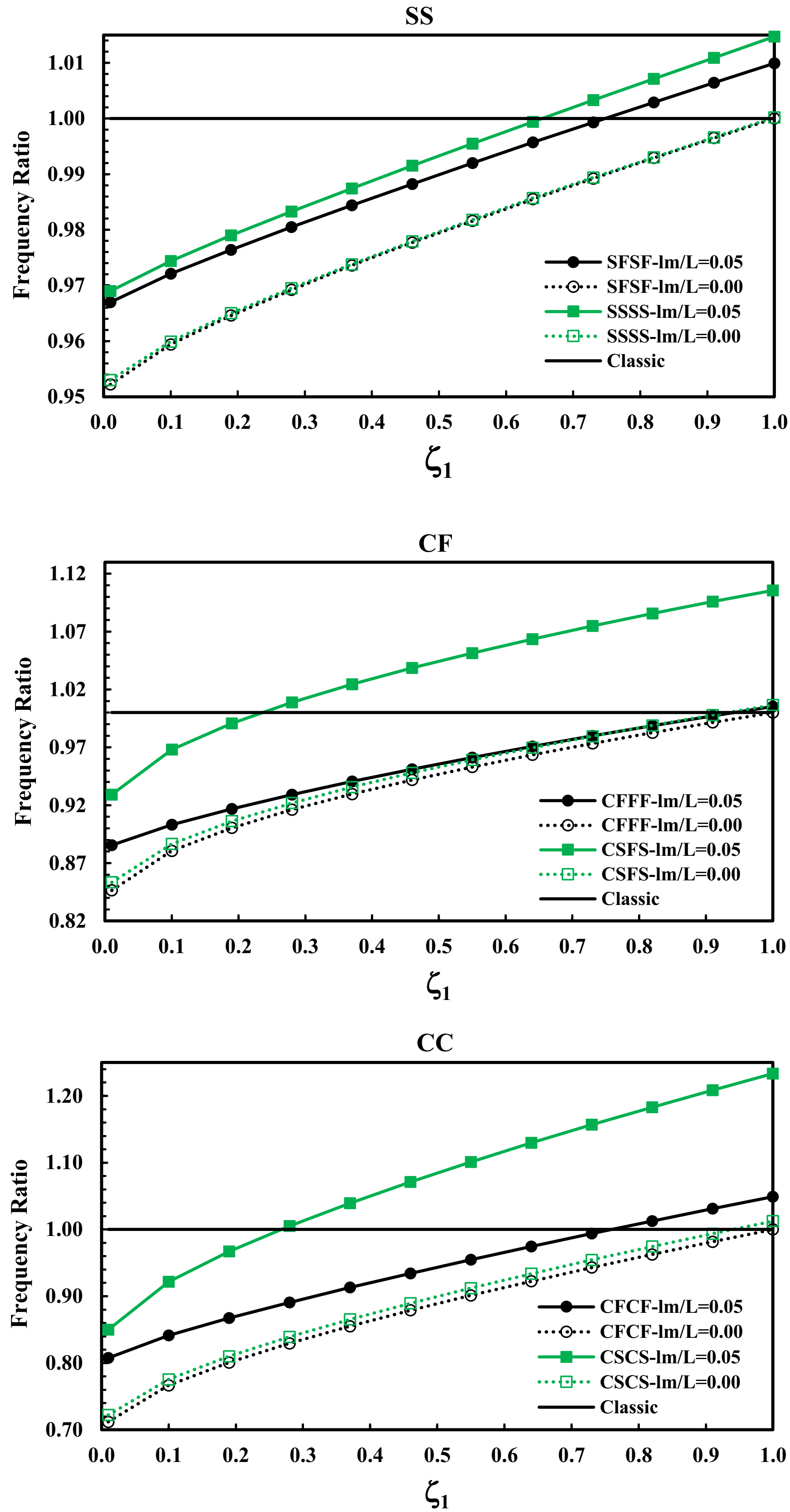

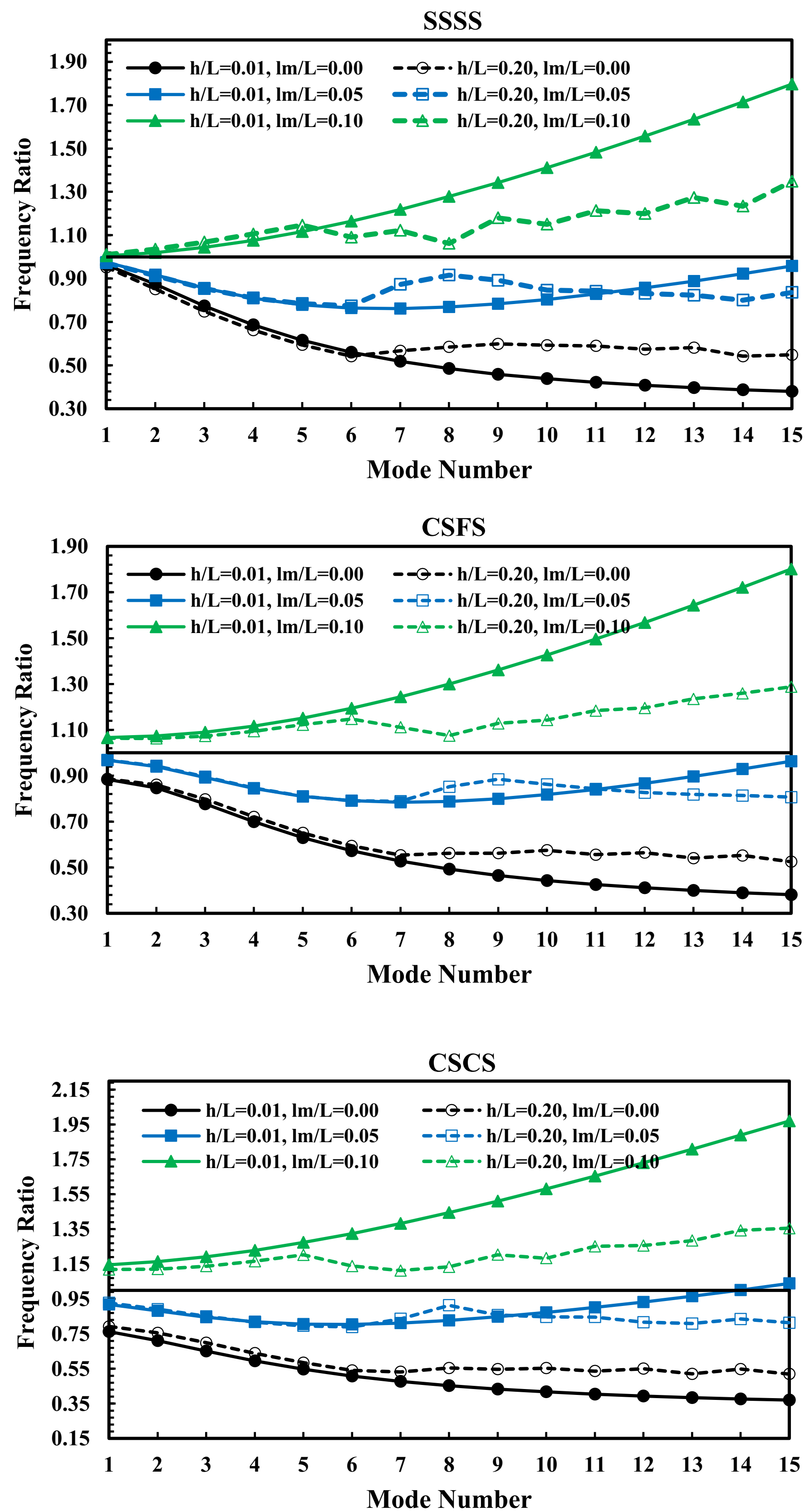

Figure. 5 Variations of frequency ratio of thin and thick LNSG nanobeams in different transverse vibration modes: $\zeta_1 = k/L = 0.10$

Table 7 Comparison between the first non-dimensional frequencies of LNSG nanobeams obtained with different beam theories, $k/L = 0.05$ and $\zeta_1 = 0.1$

BC		$h/L = 0.05$			$h/L = 0.15$		
		l_m/L			l_m/L		
		0.025	0.075	0.100	0.025	0.075	0.100
SFSF	Exact-TBT	9.75324	9.91203	10.0071	9.41946	9.58071	9.67913
	Exact-EBT	9.7981	9.9565	10.0511	9.7981	9.9565	10.0511
	Dif. (%)	0.46	0.45	0.44	4.02	3.92	3.84
SSSS	Exact-TBT	9.75639	9.97814	10.1622	9.44075	9.69881	9.89794
	Exact-EBT	9.79866	10.0152	10.1972	9.79866	10.0152	10.1972
	Dif. (%)	0.43	0.37	0.34	3.79	3.26	3.02
CFFF	Exact-TBT	3.31872	3.38955	3.42848	3.26989	3.33848	3.37615
	Exact-EBT	3.32501	3.39613	3.43523	3.32501	3.39613	3.43523
	Dif. (%)	0.19	0.19	0.20	1.66	1.73	1.75
CSFS	Exact-TBT	3.44834	3.80545	3.99801	3.3958	3.7424	3.92929
	Exact-EBT	3.45511	3.81361	4.00691	3.45511	3.81361	4.00691
	Dif. (%)	0.20	0.21	0.22	1.75	1.90	1.98
CFCF	Exact-TBT	19.8359	22.3864	24.1371	17.7782	19.7195	21.0200
	Exact-EBT	20.1500	22.8056	24.6365	20.1500	22.8056	24.6365
	Dif. (%)	1.58	1.87	2.07	13.34	15.65	17.21
CSCS	Exact-TBT	21.0843	26.2865	29.5118	18.8124	22.9695	25.5177
	Exact-EBT	21.4342	26.8171	30.1630	21.4342	26.8171	30.1630
	Dif. (%)	1.66	2.02	2.21	13.97	16.75	18.20

For $j < i$

$m = 5i-4,\ 5i-3, \ldots, 5i+4,\ 5i+5$

$n = 5j-4,\ 5j-3, \ldots, 5j+4,\ 5j+5$

$$
\begin{aligned}
knl^{ij}_{mn} = & \int_{x_j}^{x_{j+1}} \left[\frac{\alpha}{2k} \int_{x_i}^{x_{i+1}} e^{\frac{x-\bar{x}}{k}} \left(\frac{\partial^2 N^w_m}{\partial \bar{x}^2} + \frac{\partial N^\gamma_m}{\partial \bar{x}} \right) d\bar{x} \right] \left(\frac{\partial^2 N^w_n}{\partial x^2} + \frac{\partial N^\gamma_n}{\partial x} \right) dx \\
& + \int_{x_j}^{x_{j+1}} \left[\frac{\beta}{2k} \int_{x_i}^{x_{i+1}} e^{\frac{x-\bar{x}}{k}} \left(N^\gamma_m \right) d\bar{x} \left(N^\gamma_n \right) dx \right] \\
& + \int_{x_j}^{x_{j+1}} \left[\frac{l_m^2 \alpha}{2k} \int_{x_i}^{x_{i+1}} e^{\frac{x-\bar{x}}{k}} \left(\frac{\partial^3 N^w_m}{\partial \bar{x}^3} + \frac{\partial^2 N^\gamma_m}{\partial \bar{x}^2} \right) d\bar{x} \right] \left(\frac{\partial^3 N^w_n}{\partial x^3} + \frac{\partial^2 N^\gamma_n}{\partial x^2} \right) dx \\
& + \int_{x_j}^{x_{j+1}} \left[\frac{l_m^2 \beta}{2k} \int_{x_i}^{x_{i+1}} e^{\frac{x-\bar{x}}{k}} \left(\frac{\partial N^\gamma_m}{\partial \bar{x}} \right) d\bar{x} \right] \left(\frac{\partial N^\gamma_n}{\partial x} \right) dx.
\end{aligned}
\tag{57}
$$

By adding all of the knl_{mn} elements which generated by changing i and j from one to the number of applied elements (NE), the total nonlocal strain gradient stiffness matrix, *KNSG*, can be created.

In the following, the production process of the local strain gradient stiffness matrix, i.e., *KLSG*, is presented. Substituting Eq. (53) into the local strain potential energy, presented in Eq. (51), and taking the integral over the length of the beam element give the total potential energy due to local part of the jth element:

$$
\begin{aligned}
U^L_j = & \frac{\alpha}{2} \int_{x_j}^{x_{j+1}} \left[\left(\frac{\partial \gamma_j}{\partial x} + \frac{\partial^2 w_j}{\partial x^2} \right)^2 + l_m^2 \left(\frac{\partial^2 \gamma_j}{\partial x^2} + \frac{\partial^3 w_j}{\partial x^3} \right)^2 \right] dx \\
& + \frac{\beta}{2} \int_{x_j}^{x_{j+1}} \left(\gamma_j^2 + l_m^2 \left(\frac{\partial \gamma_j}{\partial x} \right)^2 \right) dx.
\end{aligned}
\tag{58}
$$

Now, the elements of *KLSG* matrix, associated with the jth element, can be generated by replacing the shape functions into the Eq. (58) and taking the derivative with respect to the degrees of freedom. Therefore:

$i = j$

$$
\begin{aligned}
kl_{mn} = & \alpha \int_{x_j}^{x_{j+1}} \left(\frac{\partial^2 N^w_m}{\partial x^2} + \frac{\partial N^\gamma_m}{\partial x} \right) \left(\frac{\partial^2 N^w_n}{\partial x^2} + \frac{\partial N^\gamma_n}{\partial x} \right) dx + \beta \int_{x_j}^{x_{j+1}} N^\gamma_m N^\gamma_n dx \\
& + l_m^2 \alpha \int_{x_j}^{x_{j+1}} \left(\frac{\partial^3 N^w_m}{\partial x^3} + \frac{\partial^2 N^\gamma_m}{\partial x^2} \right) \left(\frac{\partial^3 N^w_n}{\partial x^3} + \frac{\partial^2 N^\gamma_n}{\partial x^2} \right) dx + l_m^2 \beta \int_{x_j}^{x_{j+1}} \frac{\partial N^\gamma_m}{\partial x} \frac{\partial N^\gamma_n}{\partial x} dx.
\end{aligned}
\tag{59}
$$

Finally, to extract the mass matrix, the kinetic energy of jth element is written and then the mass matrix element is obtained as follows:

$$T = \int_{x_j}^{x_{j+1}} \frac{1}{2}\left(\rho I \phi_j^2 + \rho A w_j^2\right) dx$$
$$= \int_{x_j}^{x_{j+1}} \frac{1}{2}\left(\rho I \left(\frac{\partial w_j}{\partial x} + \gamma_j\right)^2 + \rho A w_j^2\right) dx$$
$$M_{mn} = \rho I \int_{x_j}^{x_{j+1}} \left(\frac{\partial N_m^w}{\partial x} + N_m^\gamma\right)\left(\frac{\partial N_n^w}{\partial x} + N_n^\gamma\right) dx + \rho A \int_{x_j}^{x_{j+1}} N_m^w N_n^w dx. \tag{60}$$

Here, it is helpful to note that, if the mesh distribution and nanobeam properties are uniform over the length of the nanobeam, the local stiffness and mass element matrices of all elements are similar, and therefore, they can be achieved easily by setting $j=1$ in Eq. (59) and Eq. (60).

After generation of $KLSG$ and $KNSG$ matrices, the local/nonlocal strain gradient matrix, $KLNSG$, can be produced by applying desired local phase fraction factor:

$$KLNSG = \zeta_1 KLSG + \left(1 - \zeta_1\right) KNSG. \tag{61}$$

Since the rotation is not considered as a degree of freedom in the present element, two ways are proposed for satisfying the boundary conditions with $\phi = 0$ and $\partial_x \phi = 0$. In the first one, similar to the approach utilized in Ref.[43], the penalty terms should be calculated and added to the total stiffness matrix, and in the second one, it can be considered that $\partial_x w = -\gamma$ for $\phi = 0$ and $\partial_{x,x} w = -\partial_x \gamma$ for $\partial_x \phi = 0$ in the boundaries, and therefore, the column and row associated with the γ and γ' in the boundaries should be, respectively, subtracted from the column and row of w' and w''. Next, columns and rows related to the γ and γ' must be removed.

In the last step, free vibration of LNSG Timoshenko nanobeams can be investigated by solving the following eigenvalue problem:

$$\left(KLNSG - \omega^2 M\right)\begin{Bmatrix} a_1 \\ \vdots \\ a_{dof} \end{Bmatrix} e^{i\omega t} = 0\,; dof = 5\mathrm{NE} + 5. \tag{62}$$

3 Numerical results and discussion

Before identifying the influences of applying the LNSG elasticity on the size-dependent vibrations of nanobeams, it is essential that the accuracy and correctness of the present formulations and solutions are examined. These assessments and further investigations on vibrations of LNSG nanobeams are performed by considering nanobeams with square cross section, i.e., $b=h$, and $\rho = 1, E = 1,\ \nu = 0.3$ and $k_s = 5/6$. Furthermore, to conduct a comprehensive study, several boundary conditions including simply supported (SS), clamped-free (CF), and clamped–clamped (CC) are evaluated.

Also, it should be noted that the BCs in which the boundary strains are set equal to zero are shown by “S”, while “F” means that the zero higher order stress is satisfied. For example, “CSCS” stands for a clamped–clamped beam with zero strains at both ends, while “CFCF” refers to a clamped–clamped beam with zero higher order stress in the boundaries.

First of all, in Tables 1, 2, 3, the convergence trend of the present LNSG FEM is checked by comparing the non-dimensional vibration frequencies obtained by the FE model with different number of elements and the exact ones generated by the present exact solutions. The results of Tables 1, 2, 3 are extracted for the LNSG nanobeams with $k/L=0.05$ and $l_m/L=0.1$.

Now, to compare the results of the exact solutions with the FEM ones in the cases of the boundary conditions with zero higher order stresses, $\sigma^1_{kl} = 0$, the first four vibration frequencies related to the SFSF, CFFF, and CFCF beams are computed and listed in Table 4. The FEM results of Table 4 are produced by applying 20 elements. Also, these results are provided by considering $h/L=0.10$, $k/L=0.05$, $\zeta_1 = 0.10$, and two different values of l_m/L.

Several interesting points can be taken from the results listed in Tables 1, 2, 3, 4. In all boundary conditions, there are good agreements between the FEM outcomes with the exact ones, and this confirms the consistency of LNSG theory, since the exact results are produced by solving the differential governing equations that are derived using the differential form of LNSG, while the FE model is directly constructed by the integral form of LNSG. Furthermore, the present FEM, which is constructed employing a new higher order beam element, maintains its precision in both thin and thick nanobeams. Therefore, it can be concluded that the present LNSG FEM is shear-locking-free and its convergence is desirable. Accordingly, all following results are produced from FEM with applying 20 elements.

In the following, since there is no work on the transverse vibrations of nanobeam with two-phase local/nonlocal strain gradient, the locking-free property and validity of the present FEM are more investigated by doing comparison between the present FEM results corresponding to thin beams with $h/L=0.0001$ and Euler–Bernoulli ones reported in the previous works. Therefore, in Table. 5, by assuming $l_m/L=0$, the non-dimensional frequencies of two-phase nanobeams, without strain gradient effect, are obtained for different nonlocal parameters and local phase fraction factors and then compared with the similar exact results which have been extracted by the procedure explained in Ref.[42]. Also, in Table 6, by applying a negligible value for local phase fraction factor, $\zeta_1 \simeq 0.0$, as well as considering $h/L = 0.0001$ and $l_m/L = 0.20$, the frequency ratios, defined as Eq. (63), of integral nonlocal strain gradient nanobeams are computed and compared with the results of Ref.[59]:

$$\text{frequency ratio} = \frac{\text{Size dependent frequency}}{\text{Classic frequency}}. \tag{63}$$

Tables 5 and 6 reveal that the present LNSG FE model of Timoshenko nanobeam is reliable and shear-locking-free, since, even in case of the thin nanobeams, there are good agreements between the present FEM outcomes with the results reported in the previous works. In the following, to identify how the LNSG affects the vibration of nanobeams, the frequency ratio (FR) is calculated in several cases and its variations are respectively plotted in Figs. 3, 4, 5 versus the l_m/k, ζ_1, and mode number. In Fig. 3, by considering $\zeta_1 = 0.01$ and $k/L = 0.10$, the fundamental FRs of nanobeams with different boundary conditions and thickness ratios are depicted against the values of l_m/k. Figure 3 indicates that by going from the lower values of l_m/k to the higher ones, the FR curves, which are first located below the classic line, rise, and intersect the classic line in a certain value of l_m/k, depending on boundary conditions and thickness ratio. Thus, it can be said that the softening effect of nonlocal parameter is dominant in lower l_m/k, while the stiffening effect of strain gradient becomes more influential in higher l_m/k.

Also, the differences between the FRs corresponding to zero boundary strains, for example SSSS, with the ones of zero higher order boundary stresses, for example SFSF, are insignificant for small values of l_m/k, while these differences become considerable in higher l_m/k, especially for CF and SS nanobeams. Therefore, it can be concluded that the role of how the boundary conditions associated with strain gradient are satisfied is more important in the cases with higher values of l_m/k.

To identify the influences of local phase fractions factor and strain gradient on the FRs of the LNSG nanobeams, variations of the FRs due to changes of ζ_1 are calculated for $l_m/L = 0.0$ as well as $l_m/L = 0.05$ and shown in Fig. 4. Evaluations of these results indicate that decreasing effect of nonlocality reduces when the local phase fraction factor grows. Also, considering strain gradient leads to stiffening effects and these effects are more significant in the cases with zero strains in boundaries than those associated with zero higher order boundary stresses. In addition, the clamped–clamped nanobeam shows more sensitivity to size-dependence factors than the other nanobeams, so that the lower value of FRs as well as the higher one occur in this type of nanobeam.

In the following, to study on the role of scale parameters associated with the LNSG on the different vibration modes of nanobeams, in Fig. 5, the FRs of the LNSG thin and thick nanobeams with zero strains in boundaries are displayed from the first to the fifteen mode for constant $\zeta_1 = k/L = 0.10$ and different values of h/L and l_m/L.

From Fig. 5, it is clear that the FRs corresponding to $l_m/L = 0$ have the values less than one in all boundary conditions and mode numbers. This is due to the softening effect of nonlocal parameter which its effect intensifies in the higher modes. On the other hand, the curves of $l_m/L = 0.10$ locate above the one and it can be seen that these curves rise by going to the higher modes. Accordingly, it can be said that similar to the nonlocal effect, the role of stain gradient becomes more considerable in higher vibration modes. An interesting behavior can be seen in the cases of $l_m/L = 0.05$, so that from the first mode up to a specific mode, the role of nonlocality is more than the strain gradient and therefore the FRs show reduction, while after that specific mode, the downward trends have stopped and they can even increase due to the stiffness-hardening effect resulted from the strain gradient. Comparisons between the FRs of thin and thick nanobeams disclose that the FRs of thin beams show uniform manners, while the curves of the beams with $h/L = 0.2$ have non uniform trends. Also, in most cases, thin nanobeams show more sensitivity to scale parameters than the thick ones, especially in the higher modes.

Finally, to make a comparison between the results of EBT and TBT, the first non-dimensional vibration frequencies of LNSG nanobeams with different boundary conditions are computed by means of the exact solutions and presented in Table 7. These results are extracted for different values of h/L and l_m/L as well as constant values of $k/L = 0.05$ and $\zeta_1 = 0.1$. Also, the percent of the difference, Dif. (%), between the outcomes of two beam theories is calculated and presented into Table 7.

From Table 7, it can be realized that, in all cases, the EBT produces higher frequencies than the TBT ones and theses differences intensify in the nanobeams with higher thickness ratio and stiffer boundary conditions. It is interesting to note that the difference percent depends on the l_m/L in such a way that, for the CF and CC nanobeams, the higher l_m/L values, the more discrepancy between the outcomes of EBT and TBT appears, while an opposite trend can be observed in the cases of the SS nanobeams.

4 Conclusion

Size-dependent transverse vibrations of Euler–Bernoulli and Timoshenko nanobeams are studied using the LNSG elasticity. The exact solutions and FEM are developed by two different approaches. For exact solutions, the equal differential form of LNSG is utilized to derive the differential governing equations and boundary conditions while the basic integral form of LNSG is employed to create the FE model. In addition, a new higher order shear-locking-free beam element with simple shape functions is proposed to construct a locking-free FE model of LNSG Timoshenko nanobeams. To determine the influences of nonlocality and strain gradient on the vibration of LNSG, several studies have been performed. Evaluating the results shows that:

- The softening effect of nonlocal parameter is dominant in lower l_m/k, while the stiffening effect of strain gradient becomes more influential in higher l_m/k.
- The role of how the boundary conditions associated with the strain gradient are satisfied is more important in the cases with higher values of l_m/k.
- The clamped–clamped nanobeam shows more sensitivity to LNSG size-dependence factors.
- In most cases, thin nanobeams shows more sensitivity to scale parameters than the thick ones, especially in higher modes.
- The present higher order beam element is an efficient, simple, and locking-free beam element which can be utilized in future studies in the problems of the LNSG with more complexity.

Finally, it can be stated that the consistency between the order of governing equations and number of all boundary conditions as well as agreement between the results of equal differential form of LNSG, exact solutions, and those of the integral from FEM prove that the LNSG can be a good alternative to the common nonlocal strain gradient theory which its inconsistency has been proved.

Appendix-A

Non dimensional form of CBCs related to the TBT:

$$\begin{aligned}
&\frac{1}{\Gamma_1^2\Gamma_2}((-1+\zeta_1)\Gamma_2\Gamma_4^2\partial_x\Phi-(-1+\zeta_1)\Gamma_1\Gamma_2\Gamma_4^2\partial_{x,x}\Phi- \\
&(-1+\zeta_1)\Gamma_1^2\Gamma_2(\partial_x\Phi-\Gamma_4^2\partial_{x,x,x}\Phi)+(-1+\zeta_1)\Gamma_1^3\Gamma_2(\partial_{x,x}\Phi-\Gamma_4^2\partial_{x,x,x,x}\Phi)- \\
&\Gamma_1^4(\lambda^2\partial_x\Phi+\Gamma_2(\lambda^2\overline{W}_T+\zeta_1\partial_{x,x,x}\Phi-\zeta_1\Gamma_4^2\partial_{x,x,x,x,x}\Phi))+ \\
&\Gamma_1^5(\lambda^2\partial_{x,x}\Phi+\Gamma_2(\lambda^2\partial_x\overline{W}_T+\zeta_1\partial_{x,x,x,x}\Phi-\zeta_1\Gamma_4^2\partial_{x,x,x,x,x,x}\Phi))+ \\
&(\Gamma_2\Gamma_4^2-\zeta_1\Gamma_2\Gamma_4^2)\partial_x\Phi)=0\ \ at\,\overline{x}=0
\end{aligned} \tag{64}$$

$$\begin{aligned}
&\frac{1}{\Gamma_1^2\Gamma_2}(-(-1+\zeta_1)\Gamma_2\Gamma_4^2\partial_x\Phi-(-1+\zeta_1)\Gamma_1\Gamma_2\Gamma_4^2\partial_{x,x}\Phi+ \\
&(-1+\zeta_1)\Gamma_1^2\Gamma_2(\partial_x\Phi-\Gamma_4^2\partial_{x,x,x}\Phi)+(-1+\zeta_1)\Gamma_1^3\Gamma_2(\partial_{x,x}\Phi-\Gamma_4^2\partial_{x,x,x,x}\Phi)+ \\
&\Gamma_1^4(\lambda^2\partial_x\Phi+\Gamma_2(\lambda^2\overline{W}_T+\zeta_1\partial_{x,x,x}\Phi-\zeta_1\Gamma_4^2\partial_{x,x,x,x,x}\Phi))+ \\
&\Gamma_1^5(\lambda^2\partial_{x,x}\Phi+\Gamma_2(\lambda^2\partial_x\overline{W}_T+\zeta_1\partial_{x,x,x,x}\Phi-\zeta_1\Gamma_4^2\partial_{x,x,x,x,x,x}\Phi))+ \\
&(-\Gamma_2\Gamma_4^2+\zeta_1\Gamma_2\Gamma_4^2)\partial_x\Phi)=0\ \ at\,\overline{x}=1
\end{aligned} \tag{65}$$

$$\begin{aligned}
&\frac{1}{\Gamma_1^3}((-1+\zeta_1)\Gamma_4^2(\Phi+\partial_x\overline{W}_T)-(-1+\zeta_1)\Gamma_1\Gamma_4^2(\partial_x\Phi+\partial_{x,x}\overline{W}_T)- \\
&(-1+\zeta_1)\Gamma_1^2(\Phi+\partial_x\overline{W}_T-\Gamma_4^2(\partial_{x,x}\Phi+\partial_{x,x,x}\overline{W}_T))+ \\
&(-1+\zeta_1)\Gamma_1^3(\partial_x\Phi+\partial_{x,x}\overline{W}_T-\Gamma_4^2(\partial_{x,x,x}\Phi+\partial_{x,x,x,x}\overline{W}_T))- \\
&\Gamma_1^4(\lambda^2\Gamma_3\partial_x\overline{W}_T+\zeta_1(\partial_{x,x}\Phi+\partial_{x,x,x}\overline{W}_T-\Gamma_4^2(\partial_{x,x,x,x}\Phi+\partial_{x,x,x,x,x}\overline{W}_T)))+ \\
&\Gamma_1^5(\lambda^2\Gamma_3\partial_{x,x}\overline{W}_T+\zeta_1(\partial_{x,x,x}\Phi+\partial_{x,x,x,x}\overline{W}_T-\Gamma_4^2(\partial_{x,x,x,x,x}\Phi+\partial_{x,x,x,x,x,x}\overline{W}_T)))+ \\
&(\Gamma_4^2-\zeta_1\Gamma_4^2)(\Phi+\partial_x\overline{W}_T))\ =0\ \ at\,\overline{x}=0
\end{aligned} \tag{66}$$

$$\begin{aligned}
&\frac{1}{\Gamma_1^3}(-(-1+\zeta_1)\Gamma_4^2(\Phi+\partial_x\overline{W}_T)-(-1+\zeta_1)\Gamma_1\Gamma_4^2(\partial_x\Phi+\partial_{x,x}\overline{W}_T)+ \\
&(-1+\zeta_1)\Gamma_1^2(\Phi+\partial_x\overline{W}_T-\Gamma_4^2(\partial_{x,x}\Phi+\partial_{x,x,x}\overline{W}_T))+ \\
&(-1+\zeta_1)\Gamma_1^3(\partial_x\Phi+\partial_{x,x}\overline{W}_T-\Gamma_4^2(\partial_{x,x,x}\Phi+\partial_{x,x,x,x}\overline{W}_T))+ \\
&\Gamma_1^4(\lambda^2\Gamma_3\partial_x\overline{W}_T+\zeta_1(\partial_{x,x}\Phi+\partial_{x,x,x}\overline{W}_T-\Gamma_4^2(\partial_{x,x,x,x}\Phi+\partial_{x,x,x,x,x}\overline{W}_T)))+ \\
&\Gamma_1^5(\lambda^2\Gamma_3\partial_{x,x}\overline{W}_T+\zeta_1(\partial_{x,x,x}\Phi+\partial_{x,x,x,x}\overline{W}_T-\Gamma_4^2(\partial_{x,x,x,x,x}\Phi+\partial_{x,x,x,x,x,x}\overline{W}_T)))+ \\
&(-\Gamma_4^2+\zeta_1\Gamma_4^2)(\Phi+\partial_x\overline{W}_T))=0\ \ at\,\overline{x}=1.
\end{aligned} \tag{67}$$

References

1. Lu P, Lee H, Lu C, Zhang P (2006) Dynamic properties of flexural beams using a nonlocal elasticity model. J Appl Phys 99(7):073510
2. Wang C, Zhang Y, He X (2007) Vibration of nonlocal Timoshenko beams. Nanotechnology 18(10):105401
3. Thai S, Thai H-T, Vo TP (2017) Patel VI. A simple shear deformation theory for nonlocal beams. Compos Struct 183:262–270
4. Phadikar J, Pradhan S (2010) Variational formulation and finite element analysis for nonlocal elastic nanobeams and nanoplates. Comput Mater Sci 49(3):492–499
5. Eringen AC (1972) Nonlocal polar elastic continua. Int J Eng Sci 10(1):1–16
6. Eringen AC, Edelen D (1972) On nonlocal elasticity. Int J Eng Sci 10(3):233–248
7. Eringen AC (1983) On differential equations of nonlocal elasticity and solutions of screw dislocation and surface waves. J Appl Phys 54(9):4703–4710
8. Eringen AC (2002) Nonlocal continuum field theories. Springer, New York
9. Reddy J (2007) Nonlocal theories for bending, buckling and vibration of beams. Int J Eng Sci 45(2):288–307
10. Ece M, Aydogdu M (2007) Nonlocal elasticity effect on vibration of in-plane loaded double-walled carbon nanotubes. Acta Mech 190(1):185–195
11. Thai H-T (2012) A nonlocal beam theory for bending, buckling, and vibration of nanobeams. Int J Eng Sci 52:56–64
12. Eltaher M, Emam SA, Mahmoud F (2012) Free vibration analysis of functionally graded size-dependent nanobeams. Appl Math Comput 218(14):7406–7420
13. Ebrahimi F, Barati MR, Civalek Ö (2019) Application of Chebyshev-Ritz method for static stability and vibration analysis of nonlocal microstructure-dependent nanostructures. Eng Comput. 29:1–12
14. Karami B, Janghorban M, Tounsi A (2019) Galerkin's approach for buckling analysis of functionally graded anisotropic nanoplates/different boundary conditions. Eng Comput 35(4):1297–1316
15. Sahmani S, Fattahi A, Ahmed N (2019) Analytical mathematical solution for vibrational response of postbuckled laminated FG-GPLRC nonlocal strain gradient micro-/nanobeams. Eng Comput 35(4):1173–1189
16. Romano G, Barretta R (2017) Stress-driven versus strain-driven nonlocal integral model for elastic nano-beams. Compos Part B Eng 114:184–188
17. Pinnola FP, Vaccaro MS, Barretta R, de Sciarra FM (2020) Random vibrations of stress-driven nonlocal beams with external damping. Meccanica 29:1–16
18. Challamel N, Zhang Z, Wang C, Reddy J, Wang Q, Michelitsch T et al (2014) On nonconservativeness of Eringen's nonlocal elasticity in beam mechanics: correction from a discrete-based approach. Arch Appl Mech 84(9–11):1275–1292
19. Xu X-J, Deng Z-C, Zhang K, Xu W (2016) Observations of the softening phenomena in the nonlocal cantilever beams. Compos Struct 145:43–57
20. Fernández-Sáez J, Zaera R, Loya J, Reddy J (2016) Bending of Euler-Bernoulli beams using Eringen's integral formulation: a paradox resolved. Int J Eng Sci 99:107–116
21. Romano G, Barretta R, Diaco M, de Sciarra FM (2017) Constitutive boundary conditions and paradoxes in nonlocal elastic nanobeams. Int J Mech Sci 121:151–156
22. Pisano A, Sofi A, Fuschi P (2009) Nonlocal integral elasticity: 2D finite element based solutions. Int J Solids Struct 46(21):3836–3849
23. Taghizadeh M, Ovesy H, Ghannadpour S (2016) Beam buckling analysis by nonlocal integral elasticity finite element method. Int J Struct Stab Dyn 16(06):1550015
24. Khodabakhshi P, Reddy J (2015) A unified integro-differential nonlocal model. Int J Eng Sci 95:60–75
25. Tuna M, Kirca M (2016a) Exact solution of Eringen's nonlocal integral model for bending of Euler-Bernoulli and Timoshenko beams. Int J Eng Sci 105:80–92
26. Tuna M, Kirca M (2016b) Exact solution of Eringen's nonlocal integral model for vibration and buckling of Euler-Bernoulli beam. Int J Eng Sci 107:54–67
27. Romano G, Barretta R (2016) Comment on the paper "Exact solution of Eringen's nonlocal integral model for bending of Euler-Bernoulli and Timoshenko beams" by Meral Tuna & Mesut Kirca. Int J Eng Sci 109:240–242
28. Tuna M, Kirca M (2017a) Respond to the comment letter by Romano and Barretta on the paper "Exact solution of Eringen's nonlocal integral model for bending of Euler-Bernoulli and Timoshenko beams." Int J Eng Sci 116:141–144
29. Tuna M, Kirca M (2017b) Bending, buckling and free vibration analysis of Euler-Bernoulli nanobeams using Eringen's nonlocal integral model via finite element method. Compos Struct 179:269–284
30. Eptaimeros K, Koutsoumaris CC, Tsamasphyros G (2016) Nonlocal integral approach to the dynamical response of nanobeams. Int J Mech Sci 115:68–80
31. Naghinejad M, Ovesy HR (2017) Free vibration characteristics of nanoscaled beams based on nonlocal integral elasticity theory. J Vib Control 24:1077546317717867
32. Fakher M, Rahmanian S, Hosseini-Hashemi S (2019) On the carbon nanotube mass nanosensor by integral form of nonlocal elasticity. Int J Mech Sci 150:445–457
33. Norouzzadeh A, Ansari R (2017) Finite element analysis of nano-scale Timoshenko beams using the integral model of nonlocal elasticity. Physica E 88:194–200
34. Norouzzadeh A, Ansari R, Rouhi H (2017) Pre-buckling responses of Timoshenko nanobeams based on the integral and differential models of nonlocal elasticity: an isogeometric approach. Appl Phys A 123(5):330
35. Norouzzadeh A, Ansari R, Rouhi H (2018a) Isogeometric vibration analysis of small-scale Timoshenko beams based on the most comprehensive size-dependent theory. Sci Iran 25(3):1864–1878
36. Norouzzadeh A, Ansari R, Rouhi H (2018b) Isogeometric analysis of Mindlin nanoplates based on the integral formulation of nonlocal elasticity. Multidiscip Model Mater Struct 14(5):810–827
37. Ansari R, Torabi J, Norouzzadeh A (2018) Bending analysis of embedded nanoplates based on the integral formulation of Eringen's nonlocal theory using the finite element method. Phys B 534:90–97
38. Faraji-Oskouie M, Norouzzadeh A, Ansari R, Rouhi H (2019) Bending of small-scale Timoshenko beams based on the integral/differential nonlocal-micropolar elasticity theory: a finite element approach. Appl Math Mech 40(6):767–782
39. Wang Y, Zhu X, Dai H (2016) Exact solutions for the static bending of Euler-Bernoulli beams using Eringen's two-phase local/nonlocal model. AIP Adv 6(8):085114
40. Wang Y, Huang K, Zhu X, Lou Z (2018) Exact solutions for the bending of Timoshenko beams using Eringen's two-phase nonlocal model. Math Mech Solids 24:1081286517750008
41. Zhu X, Li L (2017a) Longitudinal and torsional vibrations of size-dependent rods via nonlocal integral elasticity. Int J Mech Sci 133:639–650
42. Fernández-Sáez J, Zaera R (2017) Vibrations of Bernoulli-Euler beams using the two-phase nonlocal elasticity theory. Int J Eng Sci 119:232–248

43. Fakher M, Hosseini-Hashemi S (2020) Vibration of two-phase local/nonlocal Timoshenko nanobeams with an efficient shear-locking-free finite-element model and exact solution. Eng Comput. https://doi.org/10.1007/s00366-020-01058-z
44. Khaniki HB (2018) On vibrations of nanobeam systems. Int J Eng Sci 124:85–103
45. Fakher M, Behdad S, Naderi A, Hosseini-Hashemi S (2020) Thermal vibration and buckling analysis of two-phase nanobeams embedded in size dependent elastic medium. Int J Mech Sci 171:105381
46. Fakher M, Hosseini-Hashemi S (2020) Nonlinear vibration analysis of two-phase local/nonlocal nanobeams with size-dependent nonlinearity by using Galerkin method. J Vib Control 11:1077546320927619
47. Hosseini-Hashemi S, Behdad S, Fakher M (2020) Vibration analysis of two-phase local/nonlocal viscoelastic nanobeams with surface effects. Eur Phys J Plus 135(2):190
48. Naderi A, Behdad S, Fakher M, Hosseini-Hashemi S (2020) Vibration analysis of mass nanosensors with considering the axial-flexural coupling based on the two-phase local/nonlocal elasticity. Mech Syst Sig Process 145:106931
49. Lim C, Zhang G, Reddy J (2015) A higher order nonlocal elasticity and strain gradient theory and its applications in wave propagation. J Mech Phys Solids 78:298–313
50. Farajpour A, Farokhi H, Ghayesh MH (2019) Chaotic motion analysis of fluid-conveying viscoelastic nanotubes. Eur J Mech A/Solids 74:281–296
51. Karami B, Janghorban M (2019) Characteristics of elastic waves in radial direction of anisotropic solid sphere, a new closed-form solution. Eur J Mech A/Solids 76:36–45
52. Xiao W-s, Dai P (2020) Static analysis of a circular nanotube made of functionally graded bi-semi-tubes using nonlocal strain gradient theory and a refined shear model. Eur J Mech A/Solids 6:103979
53. Ebrahimi F, Barati MR, Dabbagh A (2016) A nonlocal strain gradient theory for wave propagation analysis in temperature-dependent inhomogeneous nanoplates. Int J Eng Sci 107:169–182
54. Ebrahimi F, Dabbagh A (2017) On flexural wave propagation responses of smart FG magneto-electro-elastic nanoplates via nonlocal strain gradient theory. Compos Struct 162:281–293
55. Zeighampour H, Beni YT, Dehkordi MB (2018) Wave propagation in viscoelastic thin cylindrical nanoshell resting on a visco-Pasternak foundation based on nonlocal strain gradient theory. Thin-Walled Struct 122:378–386
56. Li L, Hu Y, Li X (2016) Longitudinal vibration of size-dependent rods via nonlocal strain gradient theory. Int J Mech Sci 115:135–144
57. Li X, Li L, Hu Y, Ding Z, Deng W (2017) Bending, buckling and vibration of axially functionally graded beams based on nonlocal strain gradient theory. Compos Struct 165:250–265
58. Rajabi K, Hosseini-Hashemi S (2017) Size-dependent free vibration analysis of first-order shear-deformable orthotropic nanoplates via the nonlocal strain gradient theory. Mater Res Exp 4(7):075054
59. Fakher M, Hosseini-Hashemi S (2017) Bending and free vibration analysis of nanobeams by differential and integral forms of nonlocal strain gradient with Rayleigh-Ritz method. Mater Res Exp 4(12):125025
60. Barretta R, de Sciarra FM (2019) Variational nonlocal gradient elasticity for nano-beams. Int J Eng Sci 143:73–91
61. Zaera R, Serrano Ó, Fernández-Sáez J (2019) On the consistency of the nonlocal strain gradient elasticity. Int J Eng Sci 138:65–81
62. Zaera R, Serrano Ó, Fernández-Sáez J (2020) Non-standard and constitutive boundary conditions in nonlocal strain gradient elasticity. Meccanica 55(3):469–479
63. Zhu X, Li L (2017b) Closed form solution for a nonlocal strain gradient rod in tension. Int J Eng Sci 119:16–28
64. Zhu X, Li L (2017c) On longitudinal dynamics of nanorods. Int J Eng Sci 120:129–145
65. Polyanin AD, Manzhirov AV (2008) Handbook of integral equations. CRC Press, Boca Raton
66. Thota S (2019) A new root-finding algorithm using exponential series. Ural Math J 5(1):83–90